Title: STING priming during immunotherapy

Master thesis: 9 -10th Semester Medicine with Industrial Specialization
Project Period: 1st of September 2019 – 29th of May 2020

ECTS: 60

Supervisor: Emil Kofod-Olsen
Co-supervisor: Ralf Agger

Project group: 19gr9053

University: Aalborg University

Complied by:
Pamela Wiktoria Owczarska (20181373)

Number of normal pages: 47 pages
Number of pages in total: 60 pages
Characters: 11828

AALBORG UNIVERSITY
DENMARK

Contents

Abbreviations

A
APC - antigen-presenting cells
B
B2M - β-2-microglobulin gene
C
CAR - chimeric antigen receptor
CCR2 - C-C chemokine receptor 2
cDC1 - conventional type 1 DC
cDC2 - the conventional type 2 DC
CDP - common dendritic cell progenitor
cGAMP - cyclic guanosine monophosphate–adenosine monophosphate
CMP - common myeloid progenitor
CSF2 - colony-stimulating factor 2 (known also as GM-CSF)
CTLA-4 - cytotoxic T lymphocyte-associated antigen 4
CXCL - chemokine (C-X-C motif) ligand
D
DAMP - damage-associated molecular pattern
DC - dendritic cells
E
ELISA - enzyme-linked immunosorbent assay
ER - endoplasmic reticulum
F
FDA - Food and Drug Administration
G
H
HLA - human leukocyte antigen
HMG-CoA - 3-hydroxy-3-methylglutaryl-CoA
I
IDO - indoleamine 2,3-dioxygenase
IFN-α/β/γ - interferon-alpha/beta/gamma
IFNAR - interferon-α/β receptor
IKK - IκB kinase 1
IL-1/2/4/6/10/35 - interleukin 1/2/4/6/10/35
IRF3 - interferon regulatory factor 3
ISG54 - interferon-stimulated gene 54
J
K
L
LPS - lipopolysaccharides
M
MDA5 - melanoma differentiation-associated protein 5
MDSCs - myeloid-derived suppressor cells
MHC - major histocompatibility complex
MMDSCs - monocytic myeloid-derived suppressor cells
MTD - maximum tolerated dose

N

NF-κβ - nuclear factor kappa-light-chain-enhancer of activated B cells

NK cells - natural killer cells

O

P

PAMP - pathogen-associated molecular pattern

PBMC - peripheral blood mononuclear cells

PD-1 - programmed death 1

pDC - plasmacytoid DC

PD-L1/2 - programmed death 1/2 ligand

Q

R

RIG-I - retinoic acid-inducible gene I

S

SEAP - secreted embryonic alkaline phosphatase

STAT2 - signal transducer and activator of transcription 2

STING - stimulator of interferon genes

T

T-VEC - Talimogene laherparepvec

TAA - tumor-associated antigens

TAM - tumor-associated macrophages

TBK - TANK-binding kinase 1

TCR - T-cell receptor

TGF-β - transforming growth factor β

Th - T helper cells

TLR - toll-like receptor

TNF - tumor necrosis factor

TME - tumor microenvironment

Treg - T regulatory cells

TSA - tumor-specific antigens

U

V

VEGF - vascular endothelial growth factor

W

X

Y

Z

Abstract

Aim: The aim of this study was to investigate if cholesterol inhibitors nystatin and simvastatin have the capacity of increasing cGAMP stimulation of the STING signaling pathway.

Method: Human and murine dendritic cells (moDC and BMDC from mouse strains BALB/c and C57BL/6) were cultured and stimulated with cholesterol inhibitors with and without addition of the 2'3'-cGAMP, for 24 hours. Then, cells were stained and the presence of maturation markers (CD86, MHC-II or CD86, CD83 and HLA-DR) was measured by using flow cytometry. THP-1 cells (wild type and STING knockout) were cultured and differentiated into macrophages. After this process, cells were stimulated with cholesterol inhibitors and 2'3'-cGAMP for 24 hours. The supernatant from stimulated macrophages was examined with HEK-Blue™ assay, which is designed to detect secretion of IFN-I.

Results: The data from flow cytometry showed a significant difference between samples treated with nystatin only and with 2'3'-cGAMP and nystatin combined together. The significant difference appeared among results from murine cells for the presence of CD86 maturation marker. There was no significant difference among values for MHC-II marker. Simvastatin did not increase the presence of either maturation marker within murine BMDCs. From human DCs, nystatin combined with 2'3-cGAMP gave higher values than when cells were stimulated only with 2'3'-cGAMP. However, there was no significant difference observed. Simvastatin data from human cells is not clear, however, the number of results was limited. From HEK-Blue™ cells assay it was observed that THP-1 WT stimulated with 50μM of 2'3'-cGAMP, secreted IFN-I and addition of nystatin raised the IFN-I secretion. IFN-I level was also increased in samples treated with nystatin and 5μM of 2'3'-cGAMP compared to stimulation with 5μM of 2'3'-cGAMP alone.

Conclusion: Nystatin in combination with a low concentration of the 2'3'-cGAMP resulted in increased DCs maturation. From HEK-Blue™ cells assay, it can be concluded that the exogenous 2'3'-cGAMP can activate the production of IFN-I, which is the result of the STING pathway activation. The production was enhanced when cells were stimulated with 2'3'-cGAMP and nystatin. However, more studies must be conducted to fully understand the mechanism behind nystatin activity.

1. Introduction

According to the International Agency for Research on Cancer, cancer is one of the leading causes of death globally. It was estimated that cancer was responsible for 9.6mln deaths worldwide in 2018 and 18mln new cases were reported [1]. Cancer therapy is rapidly developing and aiming to become P4, meaning predictive, personalized, preventive and participatory. In order to fully become P4 new approaches in the treatment of cancer as well as new tools in diagnostics must be developed [2]. Age is one of the major factors of survival for cancer patients. In 2017, 46% of cancer deaths were among people at the age of 70 or older and 41% among people between age 50-69 [3]. Older people often suffer from other chronic conditions including heart diseases and diabetes, which make treatment more challenging and lead to prolonged recovery time. Traditional treatment such as chemotherapy carries many side effects, and elderly patients have a higher risk of experiencing serious adverse effects. Due to age factor, chemotherapy is usually not recommended as a treatment option for this patient group [4]. Risk of treating elderly patients, insufficiency of treatment and severe side effects, are the reasons why new approaches in cancer treatment are in demand.

1.1. Tumor immunology

The role of immune system (both innate and adaptive) in tumorigenesis is unquestionable. Paul Ehrlich was the first person who noticed a correlation between immune system and tumor growth. According to Ehrlich, the immune system could have an impact on tumor repression. Nonetheless, the concept of immunosurveillance was first proposed over 50 years later by Lewis Thomas and Sir Frank Mac Farlane Burnet. In 1959 Lewis Thomas pointed out that tumor cells present specific neo-antigens that can be recognized by immune cells. In the 1970s Burnet, based on Thomas' hypothesis, defined the immune surveillance theory. Immune surveillance of cancer begins with recognition of tumor-specific antigens (TSA) or tumor-associated antigens (TAA) via antigen-presenting cells (APC) such as dendritic cells, macrophages and B lymphocytes. The difference between those antigens is in their specificity of occurrence among different cell types. TSAs are present only on cancer cells and TAAs are also presented on the surface of healthy cells. However, on cancer cells, the amount of antigen is usually increased or the antigen naturally does not appear on this cell type [5]. Tumor-specific epitopes originate from TAA and TSA proteins released from dead cancer cells that were phagocytized by e.g. DCs, degraded by proteasome into short peptides and are presented on MHC I and MHC II molecules [6]. After recognition of antigen, DCs migrate to lymph nodes where they can activate T cells, including cytotoxic T lymphocytes (CTL), which infiltrate the tumor tissue and kill tumor cells by enzymatic lysis. DCs can also enhance innate immune response, by activating NK cells, which also destroy tumor cells by the same mechanisms as CTLs [7]. Since people still get cancer immune surveillance theory seemed incomplete. In early 2000s Dunn and Schreiber came up with a concept of cancer immunoediting [8]. The immunoediting theory describes dynamic relationship between tumor cells and immune system. It is divided into three phases: elimination, equilibrium, and escape. The first phase called elimination covers the immune surveillance theory where the innate and adaptive immune systems work together in order to destroy cancer cells. Cancer cells are prone to mutate and some of the mutations can help tumor to create immune resistance. Immune cells, and cytokines released by them, exert selection pressure on cancer cells and by that shapes tumor immunogenicity. This phase is called the equilibrium, it can last for years and eventually lead to the last phase, the tumor escape. Selection pressure promotes growth of cell populations with mutations, which give them the ability to hide from recognition by immune cells like DCs. After this phase, the tumor begins to be clinically apparent [9] (figure 1).

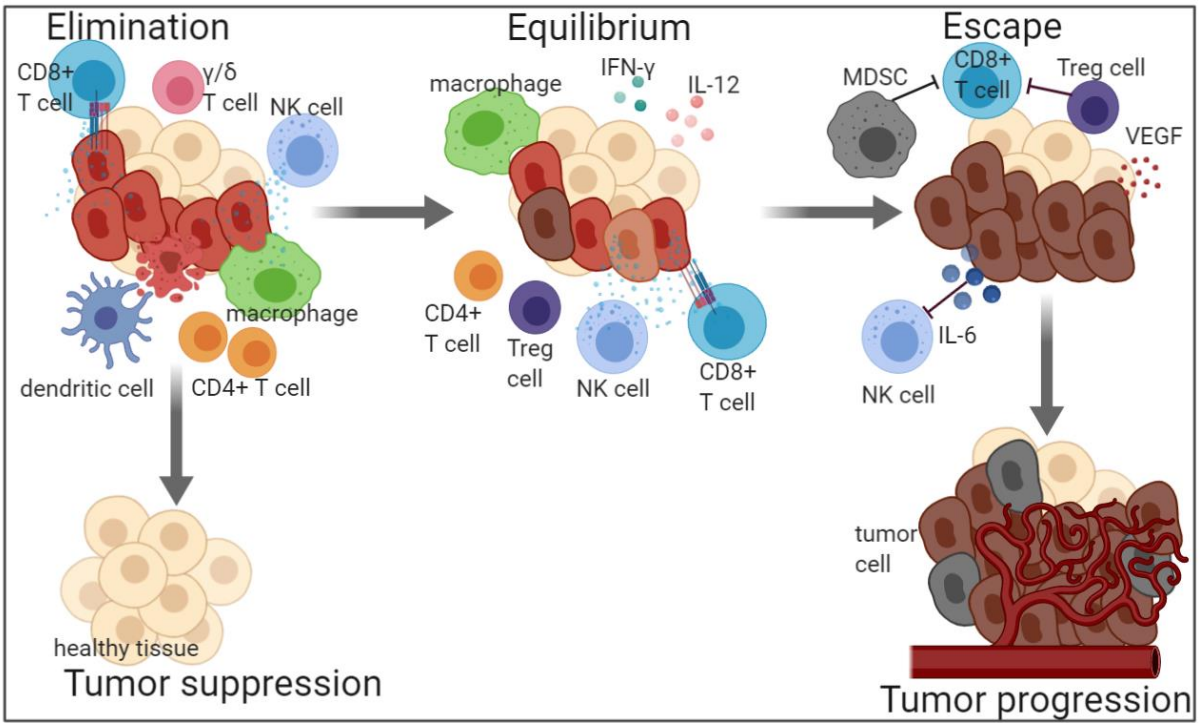

Figure 1. The concept of immunoediting. During elimination phase tumor tissue is infiltrated by immune cells. Innate and adaptive immune cells eliminate tumor cells by production of inflammatory cytokines, release of enzymes (leading to cell lysis) and recognition of tumor antigens by dendritic cells. Elimination leads to either death of all tumor cells or 2nd phase called equilibrium. Equilibrium is a balance phase between the growth of tumor and elimination of mutated cells. Tumor cells are prone to mutate and eventually, new mutations make the tumor cells resistant to immune system attack, which is the 3rd phase, escape. New blood vessels will be created to supplement tumor with oxygen, and it will lead to the spread of the tumor. Figure was made in ©BioRender.

There are several mechanisms by which cancer cells avoid an attack by immune cells.

When tumor progression occurs, changes in the function of the immune system can be seen. Effector immune cells such as plasma cells, T helper (Th) and CTLs are usually downregulated. Nonetheless, cells that inhibit the tumor suppression e.g. T regulatory cells (Treg), tumor-associated macrophages (TAM) and myeloid-derived suppressor cells (MDSCs) are often upregulated and present in the tumor tissue, where they are playing a role in formation of the suppressive tumor microenvironment (TME) [10]. This microenvironment is composed of extracellular matrix and other cell types, which are recruited by the tumor [11]. Stromal, vascular and immune cells as well as blood and lymphatic vessels can be found in tumor niche. Their function is controlled by tumor in favor to support its progression and growth [12]. Treg cells are able to produce immunosuppressive molecules, like IL-10, IL-35 and TGF-β, which leads to inhibition of effector cells [13].Tumor cells not only recruit other types of cells to produce immunosuppressive cytokines but they can also secrete some of them itself such as TGF-β, vascular endothelial growth factor (VEGF), indoleamine 2,3-dioxygenase (IDO) and galectin [9]. VEGF is essential for angiogenesis, which is required for tumor growth. New vessels supply the tumor with oxygen and nutrients. Without them, the tumor could not grow

more than 1-2 mm. [14]. The enzyme IDO catalyzes tryptophan catabolism. Breakdown of tryptophan molecules and toxic products of its metabolism including, kynurenine and quinolinic acids, lead to the death of effector T cells [15]. Galectins are a family of proteins belonging to lectins. Galectin-1 -3 and -9 have multiple functions during the escape phase. For example, the three galectins mentioned above are able to induce T cell apoptosis through different signaling pathways. The role of galectins depends on location of tumor and correlates with patient's survival prognosis [16].

Another escape mechanism that tumor cells apply is to partially or fully downregulate MHC-I receptor from their surface, which makes them resistant to recognition and destruction by cytotoxic T cells. Lack of MHC-I receptor is a result of genetic instability. The mutation occurs in the coding sequence for MHC-I heavy chain with a locus on chromosome 6 or in an exon of β-2-microglobulin gene (B2M), on chromosome 15. On the other hand, NK cells mediate killing of cells with loss of MHC-I molecules [17].

Checkpoint molecules play an important role in tumor immune resistance. Checkpoint proteins can enhance or inhibit the activity of the immune system. Some tumor cells are able to express checkpoint proteins such as CTLA-4 and PD-1 on their surface, which help them to inactivate immune responses [18]. These checkpoint proteins will be described in more detail in the section regarding cancer immunotherapy approaches.

1.2. Dendritic cells

Dendritic cells (DCs) play a role as a bridge between the innate and adaptive immune system. DCs originate from the hematopoietic cell lineage. Hematopoietic stem cells can differentiate into common myeloid progenitor (CMP) cells, which differentiate into common dendritic cell progenitor (CDP) and monocytes. CMP cell differentiation into monocytes is a multistep process, which depends on the activation of Nur77 transcription factor. The lineage of DCs is further branching from those originated from CDP cells and those differentiated from monocytes [19].

DCs originated from CDP are the conventional type 1 DCs (cDCs1), the conventional type 2 DCs (cDCs2) and the plasmacytoid DCs (pDCs). Each DCs subset differs within markers expression and functionality (table 1). There is also a subset of DCs called Langerhans cells, found in the skin area, and they will not be described further here.

Human cDCs1 is the smallest population of DCs, only ~0.05% of peripheral blood mononuclear cells (PBMCs). This subpopulation of DCs detects viral RNA by highly expressed Toll-like receptors 3 (TLR3) and TLR8. cDC1 is also a very efficient IL-12 producer and mediate CD4+ T cell maturation towards Th1 subtype. After stimulation of cDC1 with poly I:C, cDCs1 produce IFN-III, which plays a role during CTL and NK responses.

cDCs2 is a larger population of PBMCs, they are expressing TLR 2,4,5,6,8 and 9. Moreover, after detection of antigen they are good producers of proinflammatory cytokines such as tumor necrosis factor (TNFα), IL-6, IL-12, IL-23 and high level of CXCL8 chemokine [20], [21] [22]. The main difference between cDCs1 and cDCs2 is within T cells activation. cDCs1 preferably lead to activation of CD8+ T cells, whereas cDCs2 preferably lead to activation of CD4+ T cells [19].

pDCs major role is production of IFN-I after sensing viral RNA via TLR 3,8,9, RIG-I and MDA5, viral DNA via TLR7 or after activation of STING pathway. Additionally, pDCs are able to produce IFN-III, IL-6, TNFα and chemokines, especially CXCL9 and CXCL10 [23].

When inflammation occurs monocytes can differentiate into monocyte DCs (moDCs), also called inflammatory DCs. moDCs are present in tumor tissue and can be obtained *in vitro* by stimulating monocytes with medium enriched with GM-CSF (granulocyte-macrophage colony-stimulating factor) and IL-4. The role of moDCs is priming Th and CTL cells. Moreover, moDCs secrete TNFα, IL-1, IL-12 and IL-23 [19], [23].

	cDC1	**cDC2**	**pDC**	**moDC**
MOUSE	CD11b CD172a TLR1/TLR6	CD8α XCR1 Clec9a CD207(Langerin) TLR3/TLR8	B220 Ly6C PDCA.1 Siglec-H TLR7/TLR9	FcγRI CD14 FcεRI CD11b CD172 CD206
HUMAN	CD11b CD172a CD1c	CD141 XCR1 Clec9a	CD303 CD304 CD123	FcγRI CD14 FcεRI CD1a/CD1c CD172a CD206

Table 1. Dendritic cells subsets - expression markers, based on [19].

DCs are going through a maturation process, which change their metabolic and cellular functions. Immature DCs are very poor in secreting pro-inflammatory cytokines or in T cell activation. Their major role is internalization of foreign antigens by endocytosis. They capture invading pathogens as well as apoptotic and necrotic cells. Immature DCs express a high level of TLR, FcR, complement and lectin receptors. Maturation process starts when DCs detect pathogen-associated molecular pattern (PAMP) or damage-associated molecular patterns (DAMP) molecules. Mature DCs lose adhesive structure, allowing them to migrate from peripheral tissue to the lymph nodes [24]. They can be characterized by an increased expression of MHC-I and II molecules, co-stimulatory molecules including CD40, CD86 and CD83 and high level of chemokine receptor CCR7 [25]. The major role of mature DCs is priming of naive T cells and activation of T-cell mediated immunity (figure 2). In TME, DCs can mature upon detection of DAMPs and are able to cross-prime T-cells, against tumor cells.

DCs infiltration to the tumor tissue and their maturation is associated with lower tumor growth [26]. However, the TME can induce DC dysfunction. High IL-6 concentration and VEGF have a negative effect on DCs maturation and lead to DC dysfunction. IL-10, which is secreted within TME is able to generate tolerogenic DCs. There are more factors within TME that are linked with DCs dysfunction. It is crucial to fully understand the impact of TME on DCs biological function in order to use DCs as an immunotherapeutic target [27].

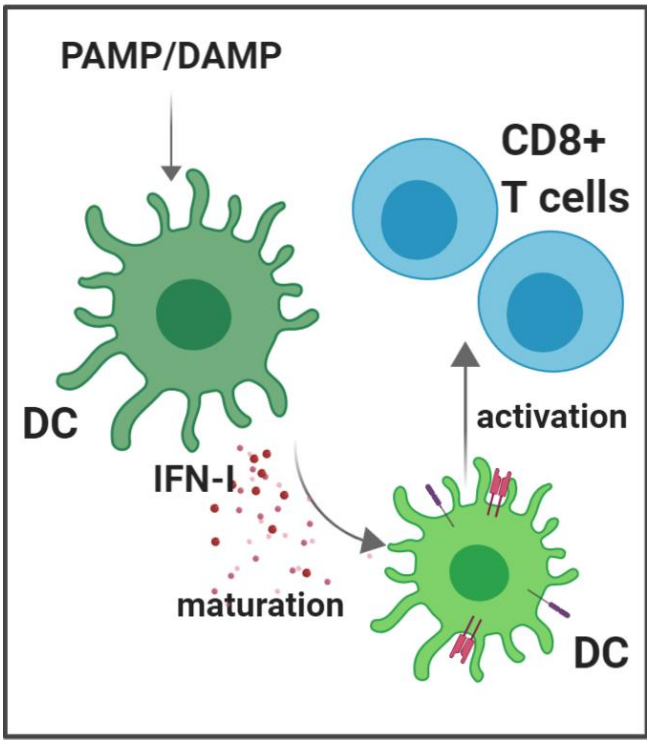

Figure 2. Maturation of DCs. Dendritic cells upon stimulatory signal produce IFN-I, which leads to maturation of other DCs. Mature DCs express a high level of molecules such as MHC-II, CD80, CD86, CD40, CD25, CD54 and CD58. After maturation DCs are able to activate CD8+ T cells. Figure was made in ©BioRender

1.3. Cancer Immunotherapy

Increased knowledge about the role of the mechanisms of immune system in inhibition of tumor growth led to the development of cancer immunotherapy as a new method of treatment. Traditional treatment of tumors includes chemotherapy, radiation and surgery. The route of treatment is determined by the type of cancer, its size and location, general health, medical history and age of the patient.

The list of side effects caused by traditional cancer treatment is long and depend on many factors (table 2).

CHEMOTHERAPY	**SURGERY**	**RADIOTHERAPY**
fatigue, nausea, bowel issues: constipation or diarrhea; hair loss (alopecia), mouth sores, loss of bone density, lower blood cell count, anxiety, depression [28]	bleeding, blood clots, higher risk of infection, discomfort and pain [29]	skin irritation, damage of exposed regions (e.g. hair loss), fatigue, nausea, vomiting, lymphedema, infertility and memory loss [30]

Table 2. Side effects of traditional cancer treatment.

Side effects and failure of traditional cancer treatment are the major reasons that press researchers to find new therapeutic approaches.

The first concept of immunotherapy in cancer came in the 19th century from William Bradley Coley. In 1891, Coley started treating bone cancer patients with lysed bacteria, which are the cause of streptococcal skin infection. He observed complete remission in 47 patients with incurable cancer. However, besides clinical success in several cancer types such as sarcoma and lymphoma, Coley's toxin did not gain a favorable opinion in medical society. The mechanism of Coley's toxin action was unknown at the time. The main disadvantage of this treatment was an injection of potentially pathogenic bacteria, which could give an additional infection for cancer patients [31]. The reappearance of cancer immunotherapy came in the 1950s, and today it has gained an increasingly important role with several types of treatments available for patients (table 3).

TYPES OF CANCER IMMUNOTHERAPY	
Passive	**Active**
Tumor-specific monoclonal antibodies	Peptide vaccines
Cytokines	DC vaccines
Adoptive Cell Transfer	Allogenic whole-cell vaccines
	Checkpoint inhibitors
	Oncolytic viruses

Table 3. Types of cancer immunotherapy [32].

1.3.1. Checkpoint inhibitors

One of the most successful immunotherapy applications is checkpoint inhibitor therapy. The achievements of James Allison and Tasuko Honjo contributed to the discovery of now FDA approved methods applying the checkpoint inhibitors, anti-CTLA-4 and anti-PD-L1 monoclonal antibodies.

Activation of T cells is a complex process where more than one signal is needed. The first signal appears when the TCR binds to MHC class I or MHC class II. This binding is also called antigen presentation because foreign antigens are displayed on the MHC molecules. Other signals can affect the response of T cells resulting in enhancement or inhibition of T cell activation.

Cytotoxic T lymphocyte-associated antigen 4 (CTLA-4) is a member of the CD28-B7 family. CD28 is a receptor on the surface of T cells, whereas B7-1 (CD80) and B7-2 (CD86) are ligands for this receptor, located on the surface of the APC. CTLA-4 competes with CD28 in binding to B7 ligand, and CTLA-4 has a higher affinity to bind B7 than CD28. CD28/B7 signal results in stimulation of T cell activation whereas CTLA-4/B7 binding blocks the activation process [33], [34]. CTLA-4 is expressed on activated Th and CTL cells but it is also found on Treg cells surface where it is expressed on a very high level [35]. In normal conditions, CTLA-4/B7 interactions fulfil the important role of regulating activation of T cells and by that maintaining T cell homeostasis.

Moreover, it was suggested that CTLA-4 is required in the negative selection of autoreactive T cells [36]. There are two drugs developed, which target CTLA-4, Ipilimumab and Tremelimumab. Both drugs are monoclonal antibodies that compete with B7 molecules for binding CTLA-4 [34].

Another checkpoint molecule is PD-1. Programmed death 1 (PD-1) is a receptor naturally occurring on the surface of effector and regulatory T cells. Like CTLA-4, PD-1 belongs to the CD28/B7 family. It binds with PD-L1 (CD274) or PD-L2 (CD273). This binding leads to suppression of cells that express PD-1 receptor such as antigen-activated T cells. PD-1/PD-L complex leads to inactivation of Zap 70, which is part of the TCR signaling pathway. One of the tumor escape mechanism is an expression of PD-L molecules, which make tumor cells able to inactivate effector T cells [37].

1.4. STING

1.4.1. Type I Interferons - role in cancer

Interferons are cytokines among which we can distinguish three types the type I including α, β, ε, κ, and ω, the type II also called IFN-γ and the type III called IFN-λ. Within the first type of IFN the most well-characterized cytokines are IFNα and IFNβ, which bind to the interferon-α/β receptor (IFNAR1 and IFNAR2) [38]. Production of type I IFN is induced after cells sense PAMP or DAMP. Most human and mouse cells express IFNAR1 or IFNAR2 on their surface. IFN type I is mainly known for its role in the antiviral response, it can inhibit virus replication, lead to host cells apoptosis and promote expression of antiviral genes in non-infected cells. IFN I plays a role in the activation of the innate and adaptive immune response, which is crucial in case of tumor immunity [25]. IFN-α is mainly produced by plasmacytoid DCs (pDCs), however, other cell types also have the ability to secrete it [38]. On the other hand, IFN-β in the TME is mainly produced by endothelial cells [39]. IFN type I play a role in many immune processes such as activation, migration and differentiation of macrophages, monocytes, T lymphocytes, B lymphocytes, NK cells and dendritic cells.

1.4.2. Induction of type I interferons

The role of interferons in suppressing tumor growth is crucial. Nonetheless, in vivo trials with IFN-I were not successful. It is worth to mention that interferons have a short lifetime so they are degraded before they can reach the target tissue [25].

It could be interesting to find an alternative way to enhance the production of interferons to be used as a therapy against infections and cancer. Different approaches have been discovered, which can result in the expression and secretion of IFN I. Among them, there are two very promising, which will be presented in this thesis. The first one is based on the activation of TLR molecules. The second approach is the activation of the stimulator of interferon genes (STING) pathway, which will be described in the next section.

During infection, the human body is able to recognize specific PAMPs, which are only associated with bacteria or viruses e.g. bacterial lipopolysaccharides (LPS) or viral RNA [40]. Moreover, biomolecules from the host organism can also be detected as a danger. DAMPs originate from injured tissue, and this group include heat-shock proteins, ATP, heparin sulfate and dsDNA among others [41]. TLRs are a group of receptors that recognize PAMPs and DAMPs. In humans, 10 types of TLRs have been identified and characterized. TLR proteins can be divided according to their location. All TLRs are membrane receptors, however, TLR1/2/4/5/6 are placed in the outer cell membrane, and TLR3/7/8/9/10 in the endosome membrane [42]. In comparison, in mice there are 13 types of TLR proteins. TLR11 also exist in human genome as a pseudogene and there is no sequence in the human genome for TLR12 and TLR13. The role of the TLR pathway is activation, maturation and control of immunological functions of immune cells, by secretion of cytokines including IFN-I. Activation of TLR pathways may also affect tumor growth, metabolism, proliferation and metastasis [43]. Although the mechanism is not fully understood, tumor cells can also express TLRs on the surface, which leads to tumor growth and higher proliferation rate [38]. There are many clinical trials that are focused on the activation of TLRs. Imiquimod is an approved therapy for a topological treatment of basal-cell cancer, which works through activation of TLR7 [43]. Other studies are focused on using different types of immunostimulants such as poly I:C to activate TLR3 [44].

1.4.3. The STING pathway

The STING pathway is a signal transmission process, which leads to IFN-I production. The STING pathway begins when the cell takes in DNA from damaged cells or from foreign origin, e.g. when a cell is infected by a pathogen. Chromosomal instability in cancer cells leads to micronuclei formation, which also activates the STING pathway [45]. In the cytoplasm, dsDNA binds to cyclic GMP–AMP synthase (cGAS). cGAS is a protein, which was discovered in 2012 by Sun and colleagues, and it works as a DNA sensor [46]. cGAS can detect dsDNA, DNA:RNA hybrids and ssDNA hairpins. Importantly, the binding affinity is determined by the length and not the DNA sequence. The binding of dsDNA triggers a change of the conformational structure of cGAS, which leads to its activation. The active cGAS enzyme catalyzes the multistep synthesis of 2'3'-cGAMP. The endogenous second messenger 2'3'-cGAMP is a compound from ATP and GTP molecules and it binds to the STING protein [47]. The STING protein plays an essential role in innate immune reactions. This 379, amino acids molecule is a transmembrane protein localized in the ER membrane. After cGAMP binding, STING traffics from the ER membrane to the ER-Golgi intermediate compartment where it activates the IκB kinase (IKK) and TANK-binding kinase 1 (TBK1). TBK1 phosphorylates interferon regulatory factor 3 (IRF3) and STING protein. Phosphorylation of STING is essential because phosphorylated STING recruits IRF3 to be activated by TBK1. IKK is degraded by ubiquitin and during this process nuclear factor kappa-light-chain-enhancer of activated B cells (NF-κβ) is released. Transcription factors (IRF3 and NF-κβ) migrate from the cytoplasm to the nucleus where they turn on the expression of IFNα, IFNβ and proinflammatory cytokines, such as IL-6, IL-1 and TNFβ [48] (figure 3).

As it was previously mentioned, activation of the STING pathway naturally occurs during infection and it plays a critical role in tumor inhibition. Studies in mice showed that IFN-I signaling is essential for tumor initiated CD8+ T cell priming. Another study conducted on mice with knockouts of the IFNAR1 and IFNAR2 genes described that cross-presentation of antigen by CD8α+ population of DCs and CD8+ T cells, was defective [49]. The STING pathway anti-tumor role was observed when the signaling was activated by endogenous tumors and it was taken into consideration as a natural immune response after radiation treatment [50], [51]. According to Hua Liang et al. the STING pathway followed by IFN-I production can be responsible for negative radiation resistance. They suggested that STING signaling takes part in MDSCs (CCR2+ subset of MMDSCs) recruitment [51]. On the other hand, Liufu Deng et al. suggest that induction of IFN-I by DCs is necessary for the anti-tumor function of CD8+ T cells [52]. The STING pathway is also able to induce cancer cells death in IFN-I independent manner. During STING signaling, expression of BAX pro-apoptotic protein is upregulated and anti-apoptotic Bcl2 protein is downregulated [50].

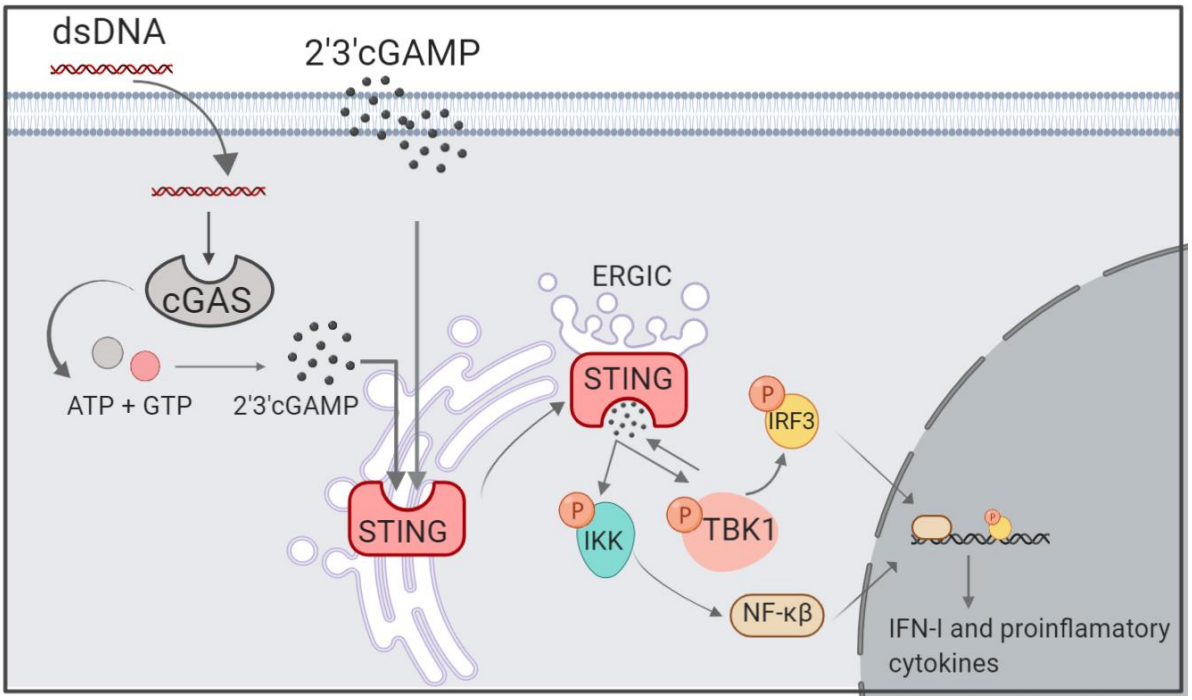

Figure 3. Activation of the STING pathway. The cGAS protein is activated by binding DNA (such as dsDNA from tumor cell). After activation, cGAS uses ATP and GTP molecules to create secondary messenger cGAMP. cGAMP binds to the STING protein, which is located on the ER membrane. Active STING protein traffics to the ER Golgi intermediate compartment (ERGIC). During translocation TBK1 and IKK proteins binds to STING and both become phosphorylated. STING-TBK1 bounding results in recruiting IRF3 protein by STING and phosphorylation of it by TBK1. IKK previously phosphorylated activates NF-κB. Dimer structure of IRF3 enters the nucleus where activates the transcription of interferon I genes. The STING protein can be also activated by the exogenous cGAMP. Figure was made in ©BioRender.

1.5. Cholesterol targeting drugs

1.5.1. Nystatin

Nystatin (C47H75NO17) is a fungistatic and fungicidal used against a variety of fungi. It is approved by the FDA for treatment of fungal infections especially with *Candida albicans*. Serious side effects have not been reported, however, it might cause inter alia nausea and gastrointestinal disturbance [53].

Nystatin belongs to the group of polyene macrolide antifungals (figure 4A) and naturally is produced by *Streptomyces spp*. It is an amphipathic molecule and contains a lactone ring with several double bonds. Nystatin creates complexes with sterols including ergosterol, which is found in fungi, and cholesterol, found in mammalian cells. The binding affinity of Nystatin is higher towards ergosterol than cholesterol, which makes nystatin an ideal antifungal drug. Above mention, barrel-like complexes create channels in the cell membrane with a diameter around 0.6 nm. Nystatin-sterol channels lead to ion leakage followed by cell death.

Nystatin toxicity depends on the composition of membrane sterols. Although, there is a hypothesis where nystatin might be active in sterols-free membranes [54].

1.5.2. Simvastatin

Simvastatin is a drug available on market under the name Zocor® (figure 4B). It is used for treatment of hypercholesterolemia and as a prevention of coronary events. Simvastatin is considered a safe drug with few to no adverse effects [55].

Simvastatin inhibits the cholesterol biosynthesis pathway. It targets the 3-hydroxy-3-methylglutaryl-CoA (HMG-CoA) reductase enzyme. This enzyme catalyzes the reduction of HMG-CoA to mevalonic acid. Mevalonic acid is a substrate in subsequent reactions leading to the synthesis of cholesterol [56].

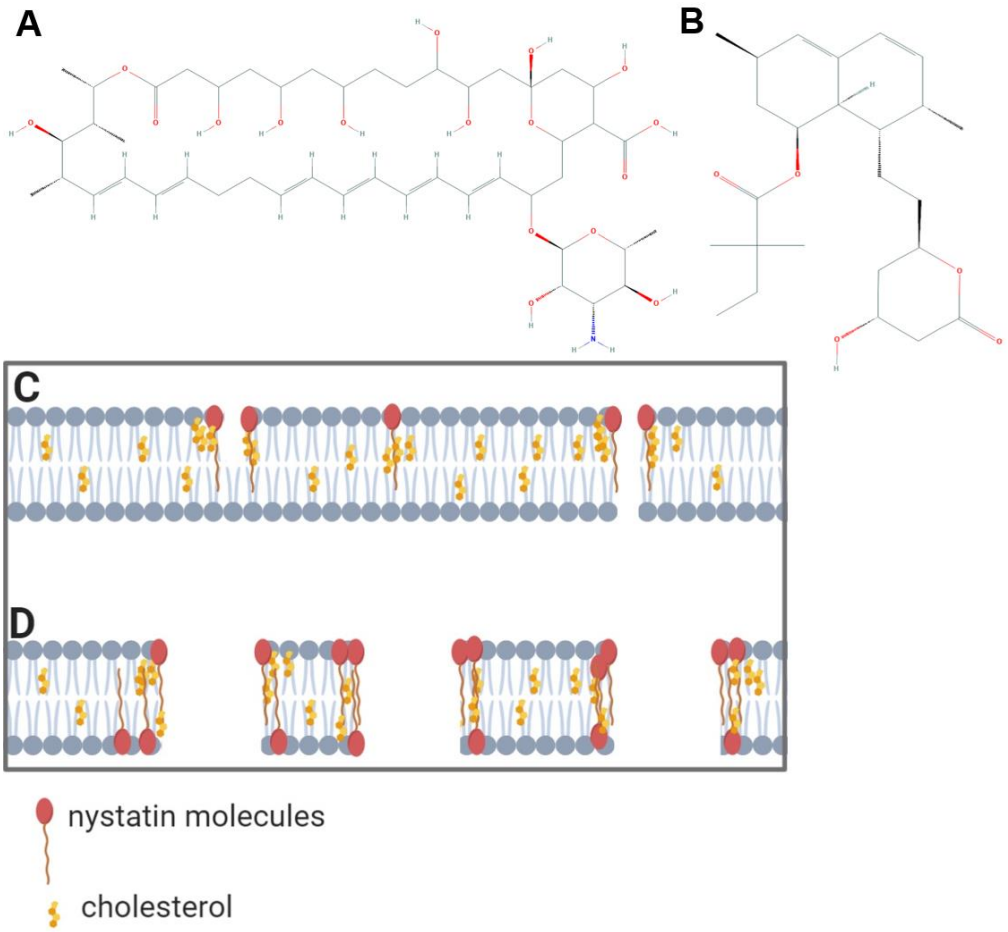

Figure 4. Cholesterol inhibitors. **A)** Chemical structure of nystatin [57] **B)** Chemical structure of simvastatin [58] **C)** and **D)** possible effect of nystatin on the cell membrane. Low concentration of nystatin **(C)** and high concentration of nystatin **(D)**. Figure was made in ©BioRender.

1.5.3. Cholesterol targeting drugs affect activation of the STING pathway

Only a few studies have been conducted on polyene macrolide antifungal antibiotics' effect on Interferon production. Borden et al. observed that combining polyene macrolides with poly I:C yields higher response in IFN production in L929 cells. They assumed that the effect must depend on the macrolide ring in their structure [59]. However, the mechanism in which polyene macrolides increase IFN production is still unknown.

Other studies focus on the inhibition of cholesterol biosynthesis and how it affects the STING pathway. STING is located on the ER membrane, which contains 3–6% of cholesterol. In 2006 Andrew Ridsdale et al. conducted a study, where they observed that depletion of cholesterol from the ER membrane impairs transport and secretion of proteins between the ER membrane and the Golgi apparatus [60]. Part of the STING pathway goes via the ERGIC where complex formation occurs, and this is needed to traffic the STING protein [61].

In 2015, York et al. hypothesized that decreased cholesterol level in the ER membrane facilitates interaction between STING and TBK1 a key protein in the STING pathway [62].

Laboratory of immunology at Aalborg University has recently shown that cholesterol blocking drugs can augment 2'3'-cGAMP stimulation in DCs. However, tested drugs Filipin-III and MβCD are not approved for treatment due to their high toxicity (unpublished).

1.6. AIM

The aim of this thesis is to evaluate how nystatin and simvastatin affects activation of the STING pathway.

During the project, it was examined whether cholesterol inhibitors (nystatin and simvastatin) could enhance the activity of the 2'3'-cGAMP molecule on DCs maturation and THP-1 macrophages activation. To evaluate it, human and murine dendritic cells were stimulated with different concentration of the two cholesterol inhibitors and 2'3'-cGAMP 24 hours prior to assessment. Maturation of DCs was analyzed via the presence of specific cell surface molecules, using flow cytometry.

To determine if cholesterol inhibitors and 2'3'-cGAMP activate the STING pathway the level of IFN-I molecules produced by THP-1 macrophages was measured via the HEK-Blue™ cell line assay.

2. Method

2.1. Cell culture

2.1.1. Human monocytes

Isolation of peripheral blood mononuclear cells (PBMCs) from peripheral blood

Donor blood was collected into four tubes with L-heparin as an anticoagulant. Afterwards, it was mixed with RPMI 1640 medium (Thermo Fisher Scientific, #52400) in a ratio of 1:1 and slowly added to tubes with 8 ml Lymphoprep (Medinor, #1114545). Subsequently, tubes were centrifuged (20 min, 20°C, 180g, acceleration: 2, break: 0), and 2 ml of the supernatant top layer was discarded. Next, tubes were centrifuged once again (20 min, 20°C, 380g, acceleration: 2, break: 0) and interphase containing PBMCs was collected. Cells were washed four times with sterile 1x PBS (Thermo Fisher Scientific #70011-036). After last centrifugation (10 min, 4°C, 300g, acceleration: 9, break: 7), cells were counted in a cell counter (Bio-Rad TC20™).

Isolation of Monocytes from PBMCs

Monocytes were isolated using the Monocyte isolation kit II from Miltenyi. After being counted, cells were transferred to a 15 ml tube, sterile PBS was added and the cell suspension was centrifuged (10 min, 4°C, 300g, acceleration: 9, break: 7). Next, the pellet was resuspended in miltenyi buffer. Subsequently, FcR Blocking Reagent, Biotin-Antibody Cocktail and Anti-Biotin Microbeads (Miltenyi, #130-091-153) were added according to the manufacturer's protocol. After incubation of PBMCs at 4°C for 15 min, 2 ml miltenyi buffer was added and the cell suspension was centrifuged (10 min, 4°C, 300g, acceleration: 9, break: 7). During centrifugation, MACS separator (Miltenyi, #130-042-302) and LS column (Miltenyi, #130-042-401) were placed on the MACS multistand (Miltenyi, #130-042-303) and the column was rinsed with 3 ml of miltenyi buffer. PBMC pellet was resuspended in 500 µl miltenyi buffer and the suspension was loaded on calibrated LS column. Next, the LS column was rinsed three times with 3 ml miltenyi buffer, and the collected suspension was centrifuged (10 min, 4°C, 300g, acceleration: 9, break: 7). The pellet containing monocytes was resuspended in 1 ml of cell culture medium and cells were counted in a cell counter.

Generation of DCs from human monocytes.

Cell density was adjusted to 1x10⁶ cells/ml and cells were seeded in 24 or 48 well plates. Human monocytes were cultured in RPMI 1640 medium with 10% of FBS (Thermo Fisher Scientific #10270-106), 2mM L-glutamine (Invitrogen, #21051-024) and 1%Penicillin/Streptomycin (Sigma-Aldrich, #P433). Cell culture medium was supplemented with cytokines: 400 IU/ml of the IL-4 (Miltenyi, #130-0930921) and 1000 IU/ml of the GM-CSF (Miltenyi, #130-093-865).

Fresh medium with cytokines was added on 3rd day of cell culture and on 6th day immature DCs were stimulated with cholesterol inhibitors and 2'3'-cGAMP (figure 5).

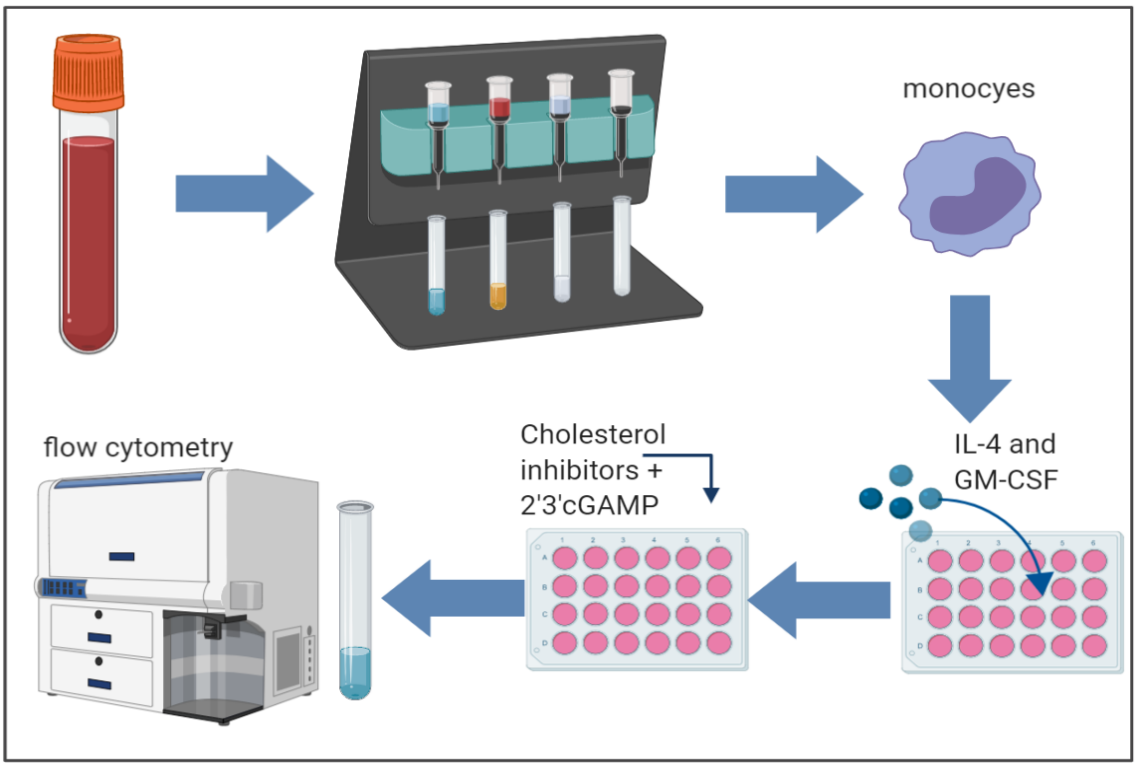

Figure 5. Generation of human dendritic cells. Figure was made in ©BioRender

2.1.2. Murine BMDCs

Isolation of murine bone marrow cells.

Mice from strains C57BL/6 and BALB/c were sacrificed, and bone marrow was harvested from femurs and tibia of each mouse. Bones were removed and cleared from the muscle tissue. Afterwards, the ends of each bone were cut off and the bone marrow was rinsed with needle and syringe filled with sterile PBS. Next, bone marrow cells were transferred to a tube and sterile PBS was added up to 50 ml. The cell suspension was centrifuged (5 min, 20°C, 300g, acceleration 9, break 7) and cells were counted in a cell counter. After counting, cells were cultured in 20 ml of a medium composed of RPMI 1640 medium with 10% of FBS (Thermo Fisher Scientific, #10270-106), 2mM L-glutamine (Invitrogen, #21051-024), 1%Penicillin/Streptomycin (Sigma-Aldrich, #P433) and 50µM β-mercaptoethanol (Sigma-Aldrich, #60-24-2). Additional cytokines were added to the growth medium: rmIL-4 in a concentration of 40ng/ml and rmGM-CSF in a concentration of 1ng/ml. Fresh medium was added on 3rd day and the medium was changed on 5th and 7th day. On 10th day, immature DCs were developed and could be used for further stimulation. When immature DCs were developed, cells were harvested by aspirating non-adherent cells from the petri dish to a 50 ml tube. The cell suspension was centrifuged (5 min, 20°C, 300g, acceleration 9, break 7) and counted in a cell counter (Bio-Rad TC20™). Cells were seeded in 24 well or 48 well plates in a concentration of 3 x 10^5 cell/well and 1.5 x 10^5 cells/well respectively with the culture medium without growth factors. Next, cells were stimulated with cholesterol inhibitors and 2'3-'cGAMP (figure 6).

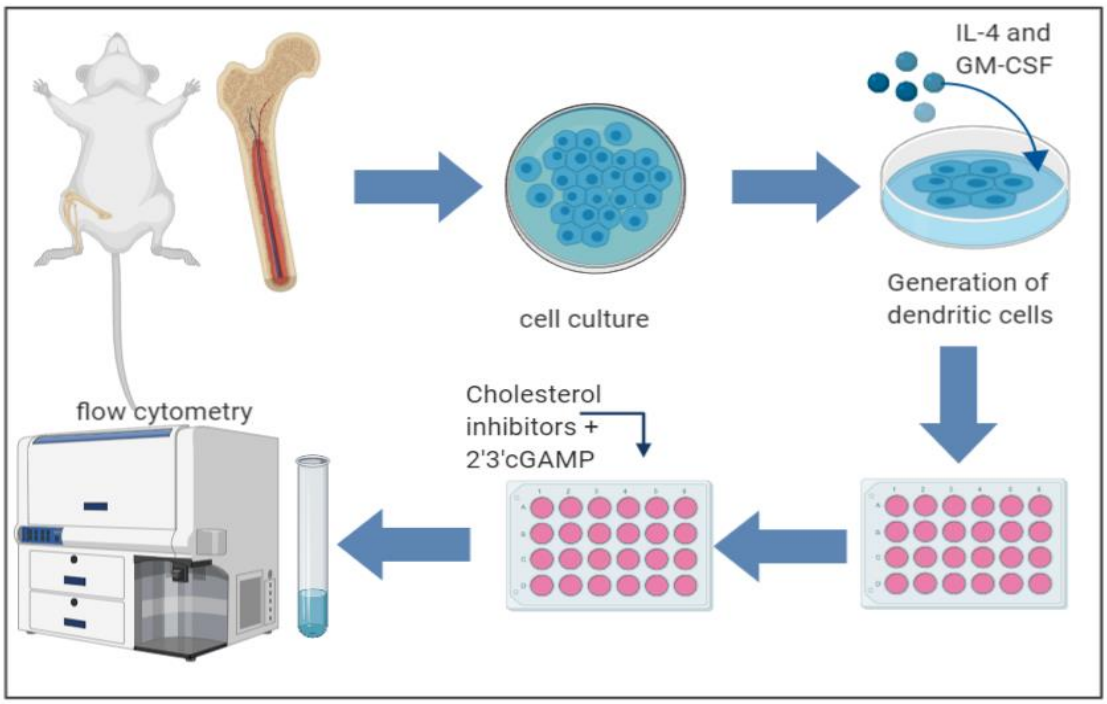

Figure 6. Murine cells (from the bone marrow of BALB/c and C57Bl/6 mice). Figure was made in ©BioRender.

2.1.3. THP-1 cells

THP-1 is a cell line of monocytes collected from peripheral blood of an infant with acute monocytic leukemia [63].
During the conducted research, two variants of THP-1 cells were used. One of the variants has knockout of the STING genes (kindly provided by Martin Roelsgaard Jakobsen, Aarhus University). The second variant is an unmodified wild type (WT).
Cells were cultured in T75 flasks in RPMI 1640 medium with 10% of FBS (Thermo Fisher Scientific #10270-106), 2mM L-glutamine (Invitrogen, #21051-024) and 1%Penicillin/Streptomycin (Sigma-Aldrich, #P433) (referred to as regular medium). THP-1 knockout cells were cultured for 48 hours. After that time the medium was changed into a selection medium [regular medium with addition of 1µg/ml of puromycin (Sigma Aldrich, #P8833)]. The selection medium was changed every two to three days and on 7^{th} day, it was replaced for a regular medium.

THP-1 cells were differentiated into macrophages by seeding them in 24 or 48 well plates and treating with 100 nM of phorbol-12-myristate-13-acetate (PMA) (Sigma-Aldrich, #16561-29-8) for 48-72 hours (figure 7).

2.1.4. HEK-blue™ IFN-α/β reported cells

HEK-Blue™ IFN-α/β cells were purchased from InvivoGen and had been generated by transfection of HEK293 cells with the human STAT2 and IRF9 genes, which are responsible for IFN-I signaling. The construct of cells contains secreted embryonic alkaline phosphatase (SEAP) gene. SEAP reporter gene is under control of ISG54 promoter, which is inducible through IFN-I. After detection of IFN-I by IFNAR1/2 receptors, the cell will synthesize SEAP protein. Presence of SEAP in the supernatant of HEKBlue™ cells can be detected, by colorimetric reaction with QUANTI-BLUE™ solution [64]
HEK-Blue™ cells were cultured in T75 flasks in the DMEM medium (Thermo Fisher Scientific, #42430025) with 10% of FBS (Thermo Fisher Scientific #10270-106), 2mM L-glutamine (Invitrogen, #21051-024), 0.5%Penicillin/Streptomycin (Sigma-Aldrich, #P433) and 100 µg/ml Normocin (Invivogen #ant-nr-1) (referred to as regular medium).
Cells were grown until they reached 70-80% confluence. To split the cells, the culture medium was aspirated, and cells were washed with sterile PBS. Trypsin (Sigma-Aldrich, #9002-07-7) was used to detach cells and cells were spun down in a centrifuge. The pellet was resuspended in a fresh medium.

After the second passage, the medium was changed into selection medium (regular medium with the addition of 30µg/ml of Blasticidin S (Sigma-Aldrich, #2079-00-7) and 100µg/ml of Zeocin (Invivogen, #11006-33-0). After two days in the selection medium, cells were detached from the bottom of the flask, by rinsing cells with warm sterile PBS and with use of a cell scraper.

For analysis of IFN-I expression, 20µl of supernatant from THP-1 cell culture was transferred to a 96 well flat bottom plate. Then 180µl of HEK-Blue™ cells (5 x 10^4 cells/well) suspension was added to each well with supernatant and cultured for 24 hours (37°C, 5% CO2).

After incubation, 20µl of the supernatant from wells of HEK-Blue™ cells culture was transferred to a new 96 well plate and 180µl of QUANTI-BLUE™ solution was added. QUANTI-BLUE™ solution was made according to the manufacturer protocol [65]. After 30 min - 6 hours of incubation (37°C, 5% CO2), absorbance was measured on the ELISA reader, Sunrise™ (wavelength = 620 nm) and the data was processed by the Magellan™ software.

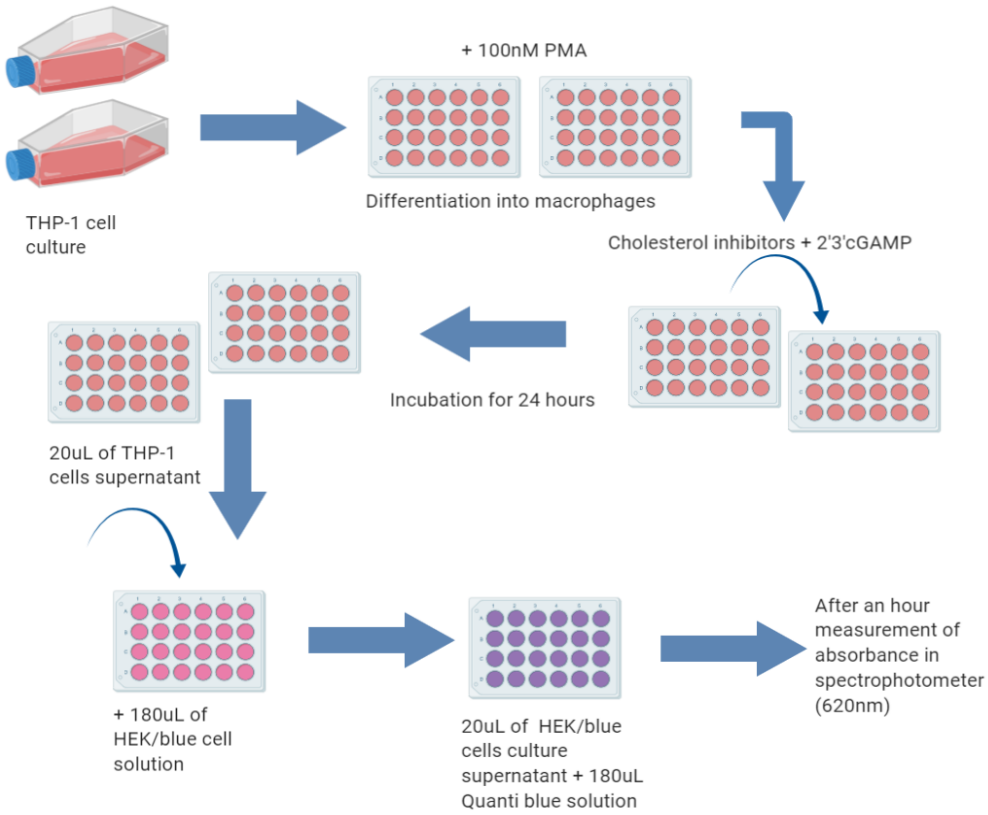

Figure 7. THP-1 cells (STING knockout cells/WT)/ HEK-Blue™ cells experiment. Figure was made in ©BioRender.

2.2. Stimulation of cells

DCs and THP-1 cells were stimulated with various concentrations of cholesterol inhibitors: nystatin (Sigma-Aldrich, #1400-61-9) and simvastatin (Sigma-Aldrich, #38956-10MG), as it is described in the result section. Before stimulation, simvastatin had been dissolved in dimethyl sulfoxide (Sigma-Aldrich, #67-68-5) to achieve a concentration of 10mg/ml. After stimulation with cholesterol inhibitors, the cells were incubated for an hour (37°C, 5%, CO2). Next, various concentrations of 2'3'-cGAMP (InvivoGen, #1441190-66-4) or 100 ng/ml of LPS were added to corresponding wells. Cells were incubated overnight (37°C, 5%, CO2), and samples were collected ~24h after stimulation.

2.3. Flow cytometry

2.3.1. Live/dead staining

Cells suspension was aspirated from wells to FACS tubes. Then 2 ml of cold 1x sterile PBS was added to the FACS tubes and the cells were centrifuged (5 min, 4°C, 300g, acceleration: 9, break: 7). After centrifugation, the supernatant was discarded and 200µl of dye solution was added. Samples with dye solution were incubated in the dark (4°C, 30min). The dye solution was composed of Fixable Viability Dye Cell Staining eFluor 780 (eBioscience, #65-0865) and 1x PBS in ratio 1:1000. After incubation samples were washed with 2 ml of sterile PBS and 2 ml of a flow buffer (PBS, 0,1%BSA and 0,01% sodium azide).

2.3.2. Single Tube Staining

Samples were washed with 2 ml flow buffer and diluted antibodies (table 4). Samples with antibodies dilutions were incubated (4°C, 30min, in the dark). After incubation samples were washed twice with the 2ml flow buffer and resuspended in 200µl of 1% formaldehyde. Fixated cells could be stored up to seven days before flow cytometry analysis. All samples were analysed on Beckman Coulter CytoFLEX s flow cytometer with lasers: 405-nm, 561-nm, 638-nm and 488-nm.

Antibody	Cat number	Host	Isotype	Reactivity	Amount of antibody	Conjugated fluorochrome
MURINE MATURATION						
anti-CD86-BV450	#48-0862-80 Invitrogen	Rat	IgG2a, κ	Mouse	0.25 µg/test	BV450
anti-MHCII-PE(I-A/I-E)	#12-5321-81 Invitrogen	Rat	IgG2b, κ	Mouse, Rat	0.02 µg/test	PE
HUMAN MATURATION						
HLA-DR-PE	#FAB4869P-100 R & D Systems	Mouse	IgG1, κ	Human	10µl/10^6 cells	PE
CD83-PE-Cy7	#561132 BD Pharmingen	Mouse	IgG1, κ	Human, Rhesus, Cynomolgus, Baboon	5µl/10^6 cells	PE-Cy7
CD86-BV421	#562432 BD Horizon	Mouse BALB/c	IgG1, κ	Human, Rhesus, Cynomolgus, Baboon	5µl/10^6 cells	BV421

Table 4. Antibodies panel for DCs maturation experiment.

2.3.3. Analysis of data

The data from flow cytometry was collected and analyzed in Kaluza software. The gating of the cells was performed as it is presented below (figure 8).

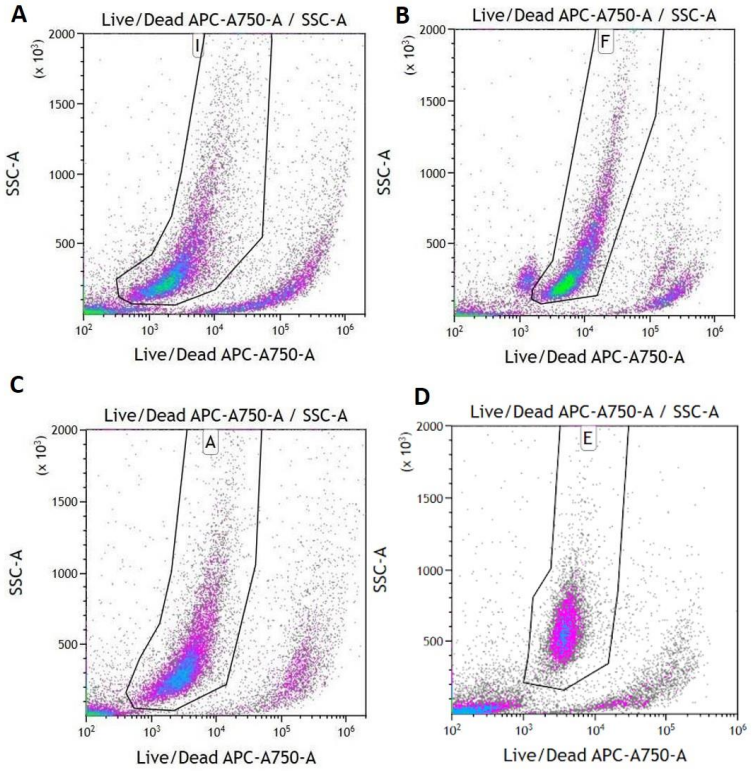

Figure 8. Example of gating strategy for DCs (murine and human cells). **A)** Gating of DCs Untreated sample (BALB/c) **B)** Gating of DCs Nystatin 31,2U/ml + cGAMP 5uM (BALB/c) **C)** Gating of DCs Nystatin 15U + cGAMP 5uM (C57BL/6) **D)** Gating of DCs Nystatin 31,2U/ml + cGAMP 5uM (human)

2.3.3.1. Statistical analysis of the data

Selected statistical comparisons were performed between samples treated with 5μM of 2'3'-cGAMP and cells stimulated with both 5μM of 2'3'-cGAMP and cholesterol inhibitor (different concentration of nystatin or simvastatin). Statistical analysis was done on GraphPad Prism 8.4.1 software with the use of the nonparametric Mann-Whitney test; P-value < 0.05.

3. Results

3.1. Dendritic cell maturation

3.1.2. cGAMP and cholesterol inhibitor induced maturation of BALB/c derived dendritic cells

Recently, it has been shown that cells can take up extracellular cGAMP through the SLC19A1 receptor and expose it in the cytoplasm [66]. In order to determine if murine DCs could mature in response to cGAMP uptake, BMDCs from BALB/c mice were stimulated with different concentrations of 2'3'-cGAMP for 24 hours.

The samples were investigated for the presence of maturation markers CD86 and MHC-II using flow cytometry.

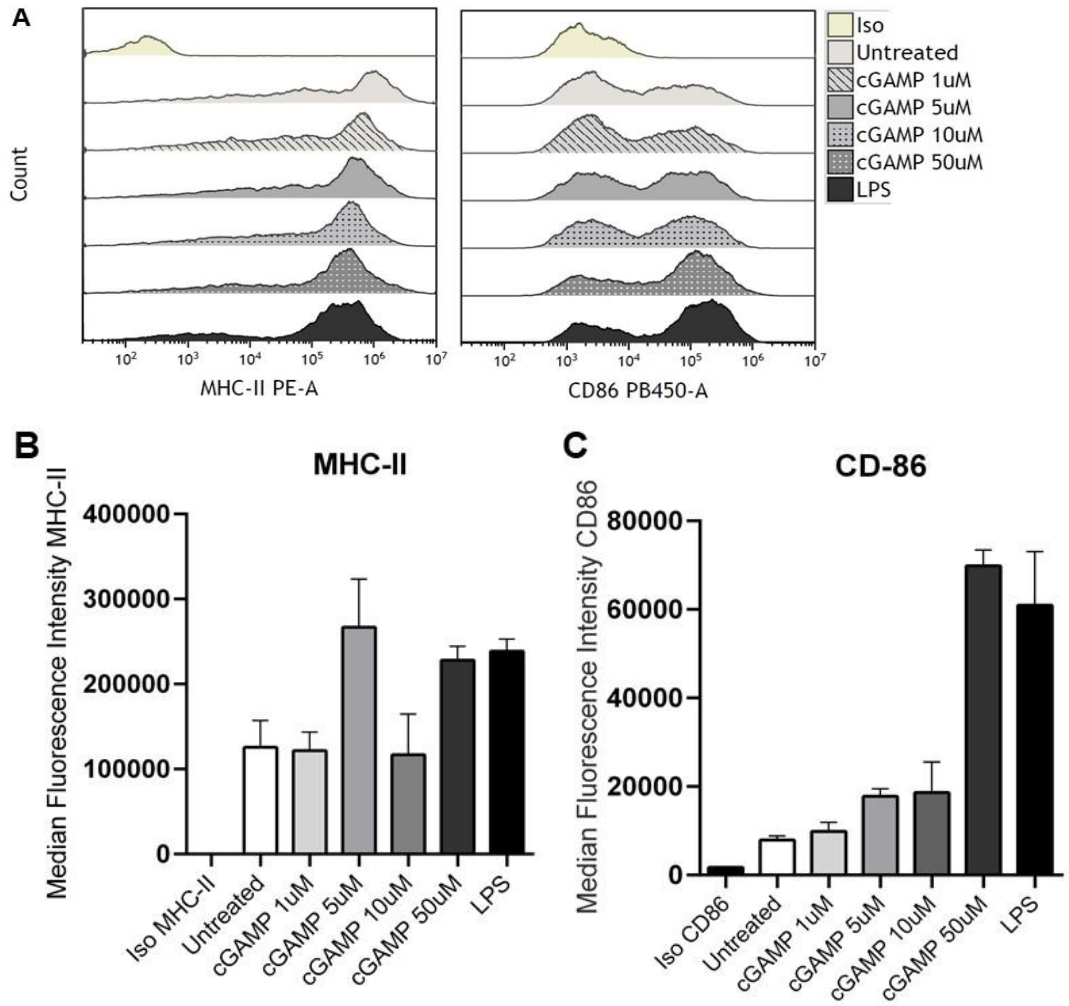

Figure 9. cGAMP induced BMDCs maturation. **A)** Flow cytometry analysis of maturation markers MHC-II and CD86 after dendritic cell stimulation with different concentrations of 2'3'-cGAMP (example of histograms from one experiment). **B)** and **C)** Bar charts of median fluorescence intensity. The data is an average from three independent experiments. The error bars present the standard error of the mean of the collected data.

When the DCs are stimulated two populations of cells can be distinguished. The first population represents cells with a low amount of maturation marker on their surface. The second population of cells, represents cells with a higher number of the marker as maturation occurred. It can be observed that the second population of cells is larger when they were stimulated with 50μM of 2'3'-cGAMP, which is consistent with results presented on bar charts (figure 9A).

The highest median fluorescence intensity for antibodies directed against the MHC-II molecule was observed for samples of cells treated with 5μM and 50μM of 2'3'-cGAMP, where the values are comparable with the sample treated with LPS (figure 9B).

For the CD86 marker of DCs maturation, the sample treated with 50μM of 2'3'-cGAMP has obtained the highest value, which is comparable with sample stimulated with LPS. The rest of the peaks from experimental samples is placed close to the level of the untreated sample peak (figure 9C).

Data collected at the laboratory of immunology, Aalborg University, has indicated a link between DCs cholesterol levels and STING activity (unpublished data). Therefore, it was set out to investigate if clinically approved cholesterol inhibitors nystatin and simvastatin could augment the maturation effects of 2'3'-cGAMP. Initially, BMDCs were stimulated with varying concentrations of nystatin and simvastatin, followed by a low concentration of 2'3'-cGAMP (5 μM). The expression of DCs maturation markers CD86 and MHC-II was analyzed by using flow cytometry.

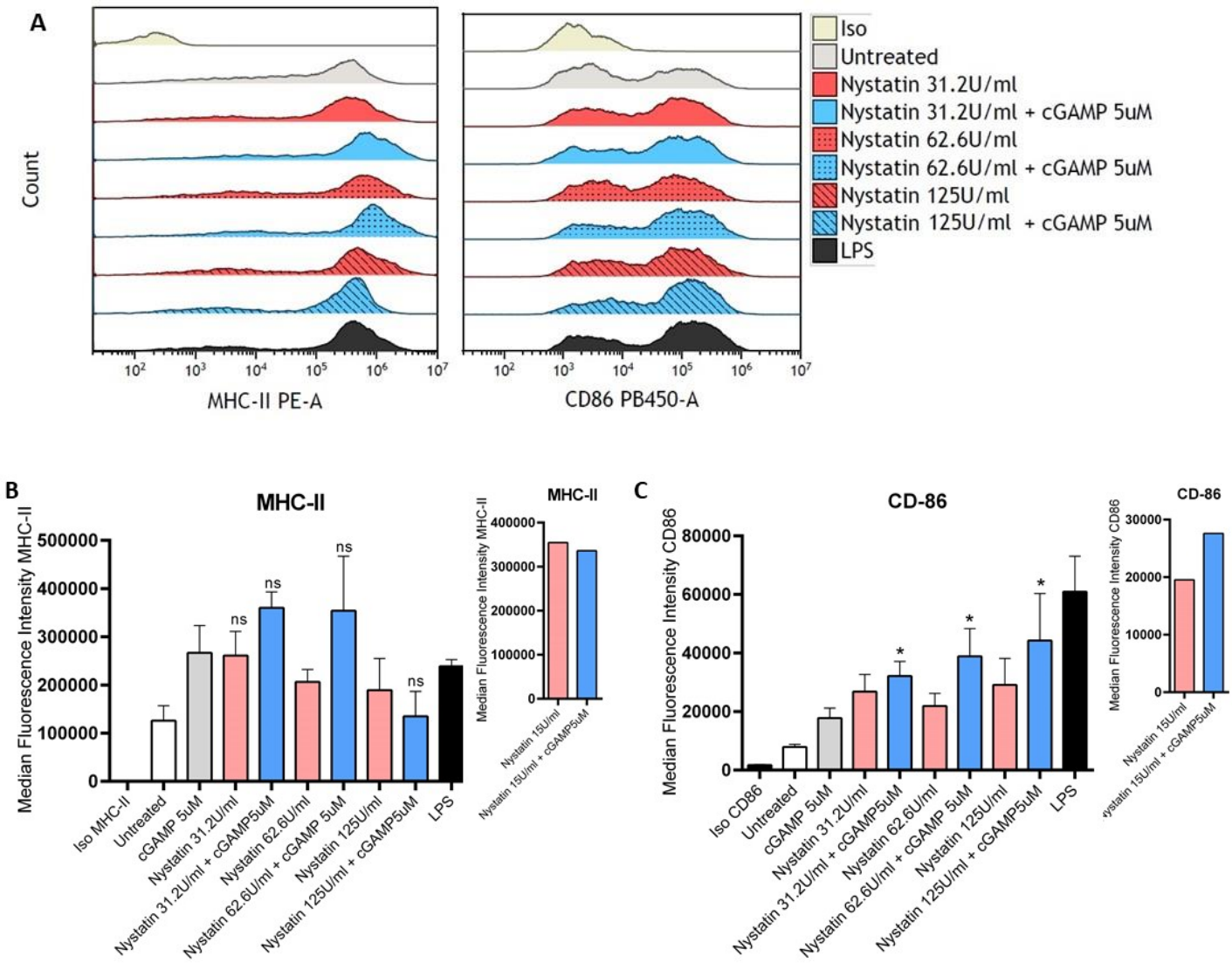

Figure 10. Nystatin and cGAMP effect on BMDCs maturation. **A)** Flow cytometry analysis of maturation markers MHC-II and CD86 after dendritic cell stimulation with different concentrations of 2'3'-cGAMP (example of histograms from one experiment). **B)** and **C)** Bar charts of median fluorescence intensity. The data is an average from three independent experiments. The error bars present the standard error of the mean of the collected data.
*Results from samples called 'Nystatin 15U/ml' and 'Nystatin 15U/ml + cGAMP 5uM' were collected only from one experiment and statistical analysis was not performed on those samples.

The highest fluorescence intensity for MHC-II marker can be observed for samples treated with 5μM of 2'3-'cGAMP in combination with nystatin (concentrations 15U/ml, 31.2U/ml and 62.6U/ml) or without an addition of the cholesterol inhibitor. The peak from 5μM of 2'3'-cGAMP sample is on a similar level as the peak of the sample treated with LPS. There was no significant difference between experimental samples (nystatin + 5μM 2'3'-cGAMP) and 5μM of 2'3-'cGAMP (figure 10B).

The results from the median of fluorescence intensity for CD86 marker show significant difference between samples treated only with 5μM 2'3-'cGAMP and in combination with nystatin (concentrations 31.2U/ml and 62.6U/ml and 125U/ml) (figure 10C).

Nystatin stimulation indicated that cholesterol inhibitors may have effect on cell maturation. Therefore, further experiments were setup to examine another cholesterol inhibitor called simvastatin in order to observe whether its presence also contributes to raising maturation markers level. Cells were stimulated with 1μM, 5μM, 10μM and 20μM of simvastatin with or without the addition of 2'3'-cGAMP (5μM) (figure 11A and B)

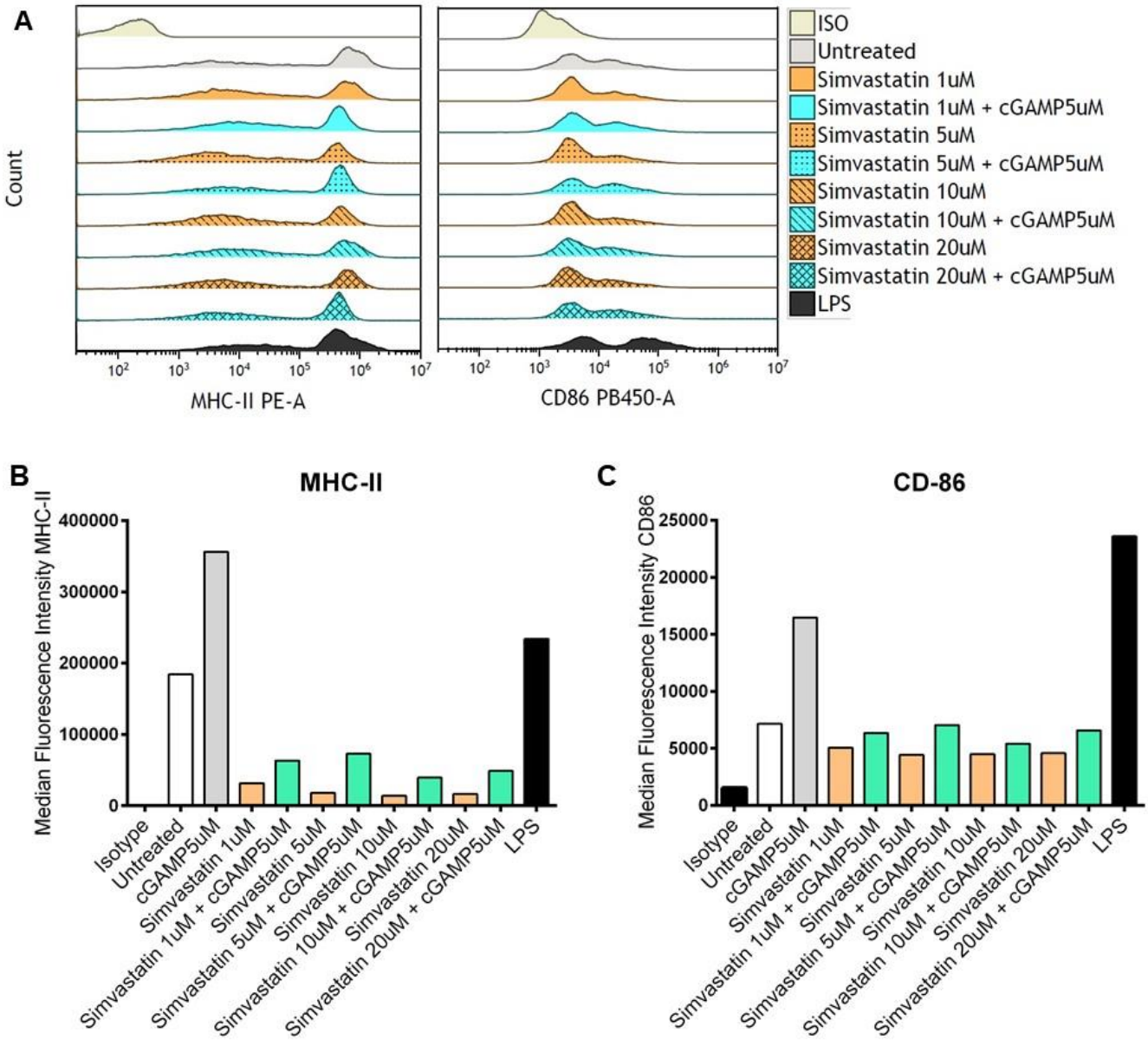

Figure 11. Simvastatin and cGAMP effect on BMDCs maturation. **A)** Flow cytometry analysis of maturation markers MHC-II and CD86 after dendritic cell stimulation with different concentrations of simvastatin and its combination with 5μM of 2'3'-cGAMP (example of histograms from one experiment). **B)** and **C)** Bar charts of median fluorescence intensity. Because the data is collected from one experiment, statistical analysis was not performed.

Bar charts from BMDCs stimulation with simvastatin show that this cholesterol biosynthesis inhibitor did not increase the number of maturation markers on the cell surface. Moreover, the peaks from samples treated with simvastatin with 2’3’-cGAMP are lower than when stimulated only with 2’3’-cGAMP (figure 11). Results of median fluorescence intensity for MHC-II marker showed that the peak of BMDCs untreated sample is higher than peaks from samples stimulated with simvastatin (figure 11B).

3.1.3. cGAMP and cholesterol inhibitor induced maturation of C57BL/6 derived dendritic cells

Since DCs stimulated with nystatin brought a positive outcome on cells originated from BALB/c mice. It was interesting to examine whether nystatin also has effect on cells from other mice strains. For this purpose, bone marrow cells from C57BL/6 mouse strain were collected, differentiated into DCs and afterwards stimulated with cGAMP and cholesterol inhibitors.

To verify that DCs from C57BL/6 also respond to pure 2'3'-cGAMP, BMDCs from C57BL/6 mouse were stimulated with its various concentrations and analyzed with use of flow cytometry.

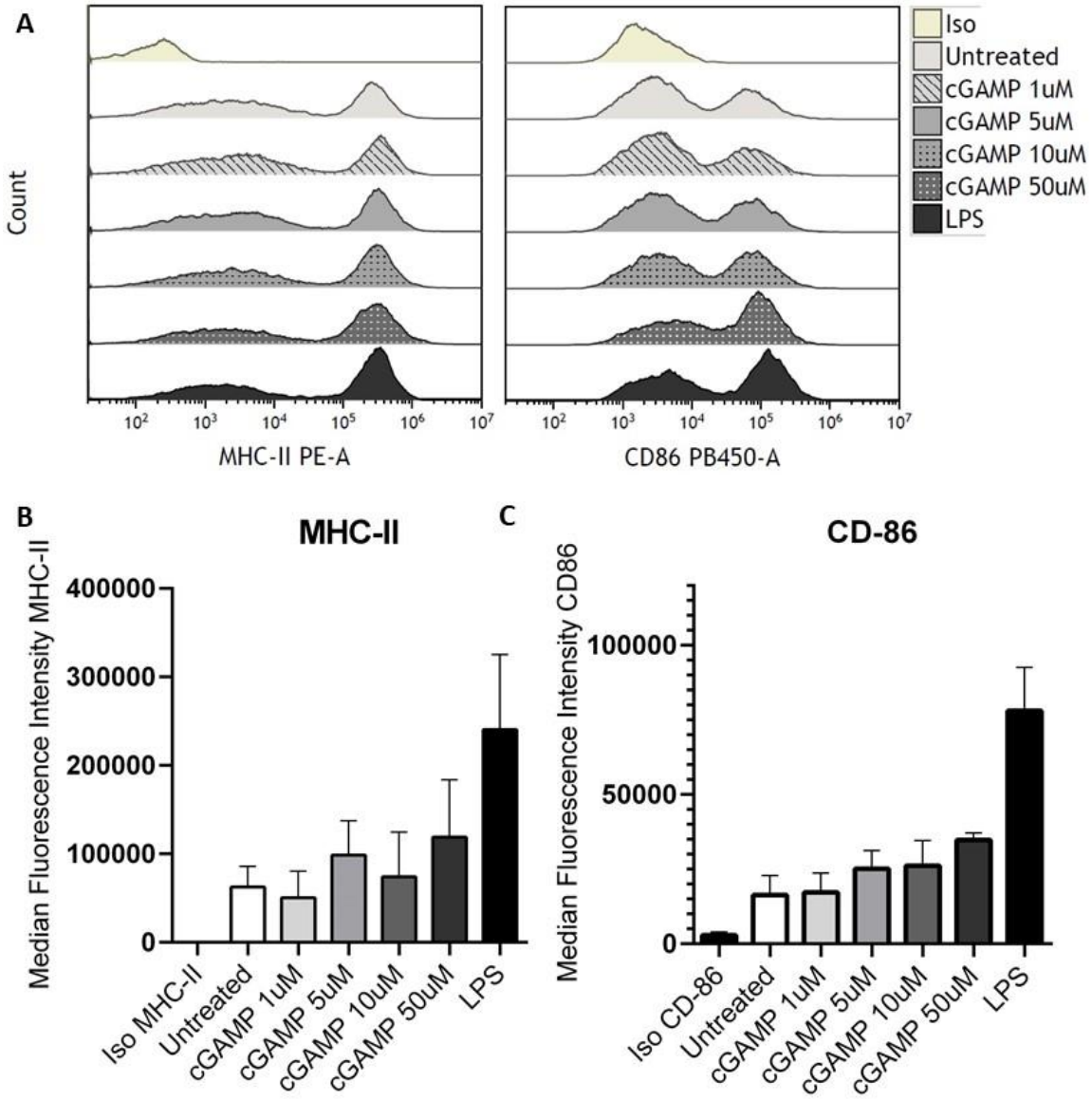

Figure 12. cGAMP induced BMDCs maturation. **A)** Flow cytometry analysis of maturation markers MHC-II and CD86 after dendritic cell stimulation with different concentrations of 2'3'-cGAMP (example of histograms from one experiment). **B)** and **C)** Bar charts of median fluorescence intensity. The data is an average from three independent experiments. The error bars present the standard error of the mean of the collected data.

Median fluorescence intensity for both markers MHC-II and CD86 presents a similar outcome. The highest peak, among samples treated with different concentrations of 2'3'-cGAMP, is for one treated with 50μM. However, none of the cGAMP treated samples are similar to the LPS value (figure 12B and C).

Due to the fact, that all concentrations used in an experiment on cells from BALB/c mice, showed similar outcome for experiment with cells from C57BL/6 mice concentrations of nystatin were decreased. Therefore, BMDCs from C57BL/6 strain were stimulated with nystatin in concentration from 5U/ml up to 30U/ml with and without the addition of 5μM of 2'3'-cGAMP.

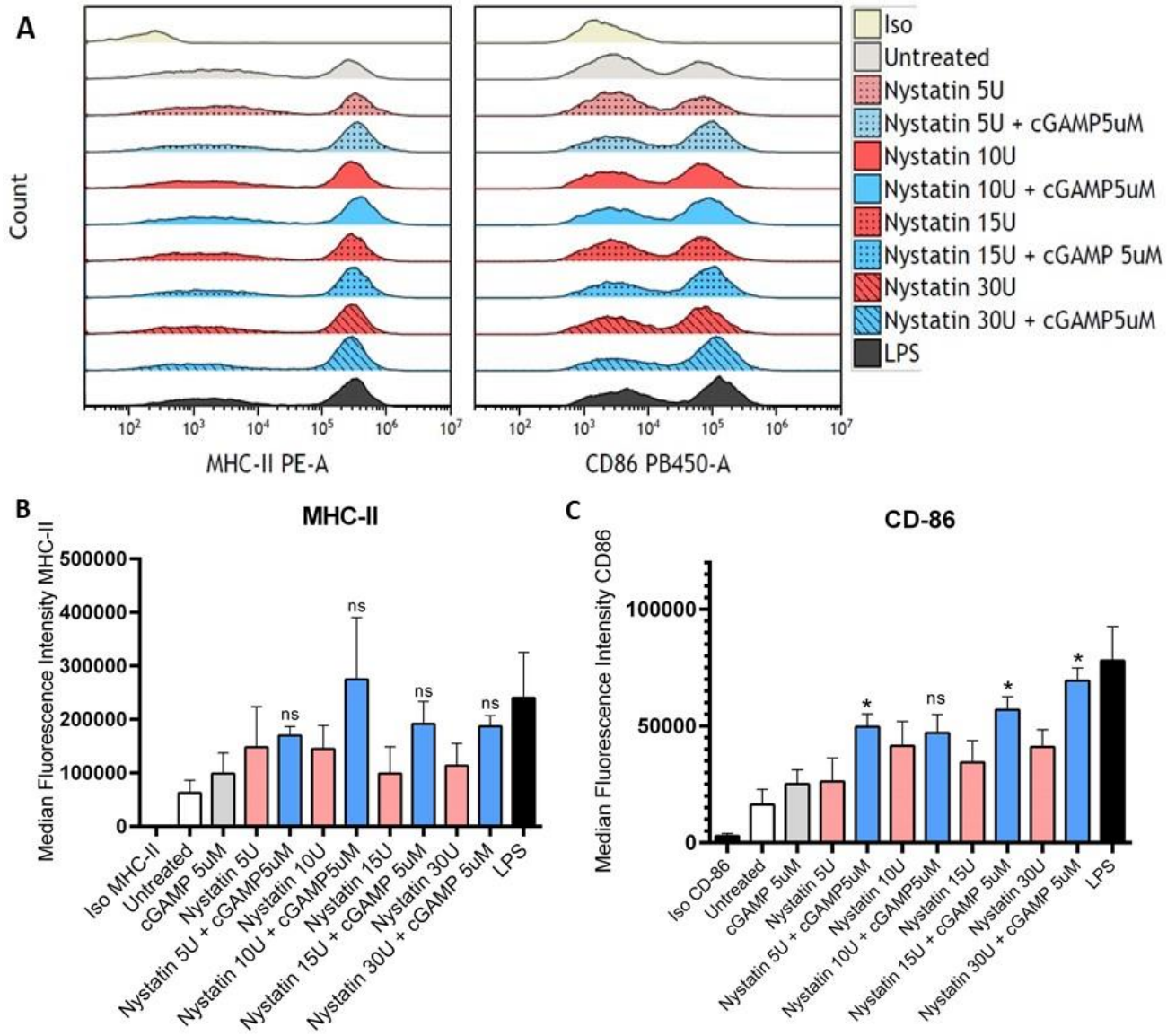

Figure 13. Nystatin and cGAMP effect on BMDCs maturation **A)** Flow cytometry analysis of maturation markers MHC-II and CD86 after dendritic cell stimulation with different concentrations nystatin and its combination with 5μM of 2'3'-cGAMP (example of histograms from one experiment). **B)** and **C)** Bar charts of median fluorescence intensity. The data is an average from three independent experiments. The error bars present the standard error of the mean of the collected data.

Histograms represent comparison in the intensity of fluorescence for maturation markers of DCs samples, treated with nystatin, its combination with 5μM of 2'3'-cGAMP and an untreated sample. It can be observed that the addition of 5μM 2'3'-cGAMP resulted in an increased population of DCs with a higher number of MHC-II and CD86 molecules (figure 13A)

There was no significant difference between samples stimulated with 5μM 2'3'-cGAMP in combination with any nystatin concentration. However, visually there a difference between the levels (figure 13B).

Values of fluorescence intensity median for the CD86 marker show a significant difference between experimental samples (nystatin in the concentration of 5U/ml, 15U/ml, 30U/ml with 5μM of 2'3'-cGAMP) and sample only stimulated with 5μM 2'3'-cGAMP (figure 13C).

Due to the high toxicity of simvastatin in concentrations used during the experiment with BMDCs from BALB/c mouse it was decided to decrease the dosage of it (figure s2). Therefore, during this attempt cells were stimulated with 0.1μM, 0.5μM and 1μM of simvastatin with or without the addition of 2'3'-cGAMP (5μM).

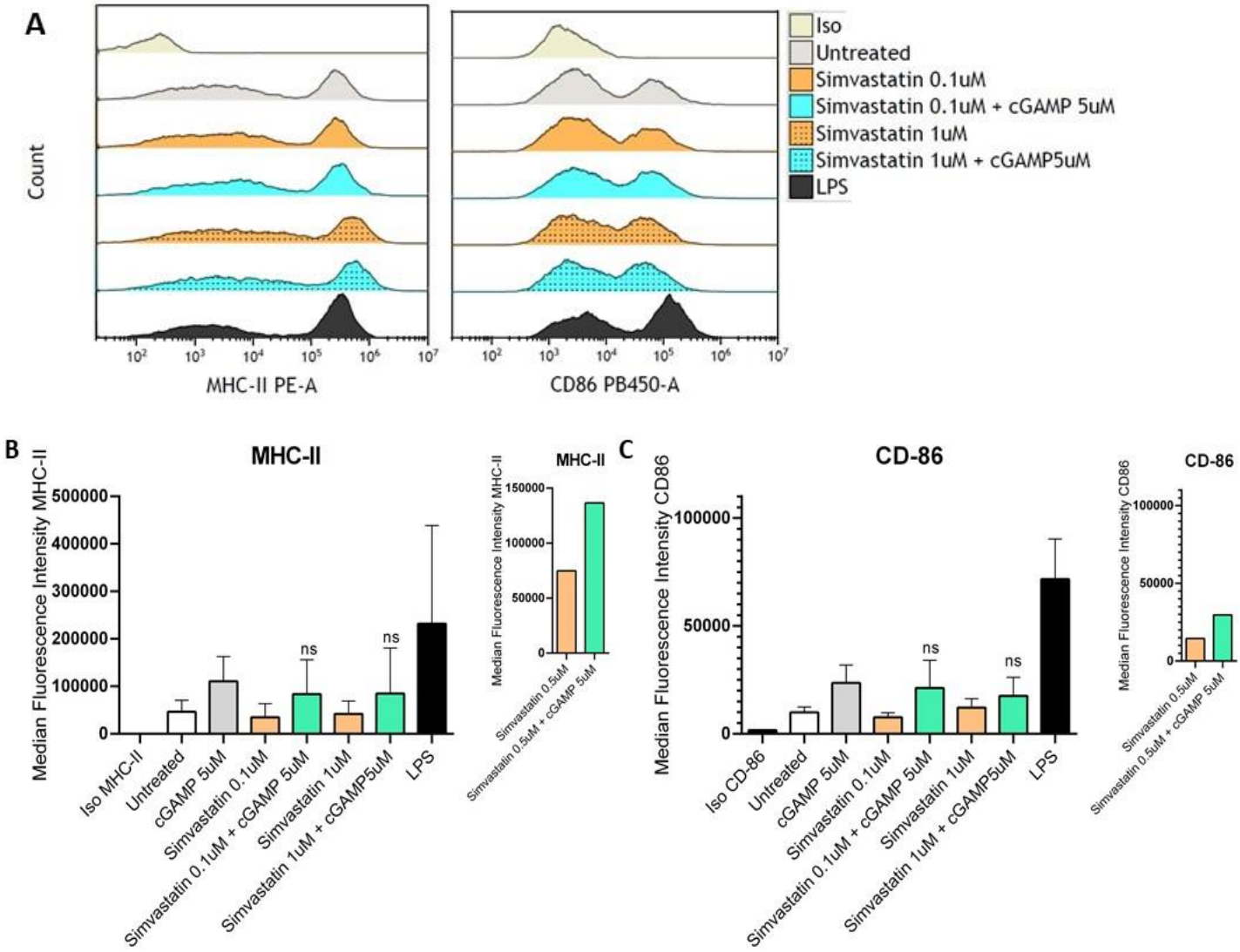

Figure 14. Simvastatin and cGAMP effect on BMDCs maturation. **A)** Flow cytometry analysis of maturation markers MHC-II and CD86 after dendritic cell stimulation with different concentrations simvastatin and its combination with 5μM of 2'3'-cGAMP (example of histograms from one experiment) **B)** and **C)** Bar charts of median fluorescence intensity. The data is an average from two independent experiments. The error bars present the standard error of the mean of the collected data.
*Results from samples called 'Simvastatin 0.5uM' and 'Simvastatin 0.5uM + cGAMP 5uM' were collected only from one experiment and statistical analysis was not performed on those samples.

The histograms show that population of cells with a low number of maturation markers (especially the CD86) is larger when cells were treated with simvastatin in comparison to values when cells were stimulated with LPS (figure 14A).

Bar charts from simvastatin experiment show that no significant difference for any of the maturation markers could be observed. Peaks from experimental samples are at a similar or lower level than a peak, which presents the value of a sample treated with 5μM of 2'3'-cGAMP (figure 14B and C).

3.1.4. cGAMP and cholesterol inhibitor induced maturation of monocyte derived dendritic cells

Due to the fact, that mouse and human cells are not identical both cholesterol inhibitors and the 2'3'-cGAMP were examined on human DCs differentiated from monocytes. The purpose was to observe whether human DCs are sensitive at the same level as murine cells. In the first stage, cells were stimulated with 2'3'- cGAMP at different concentrations (figure 15).

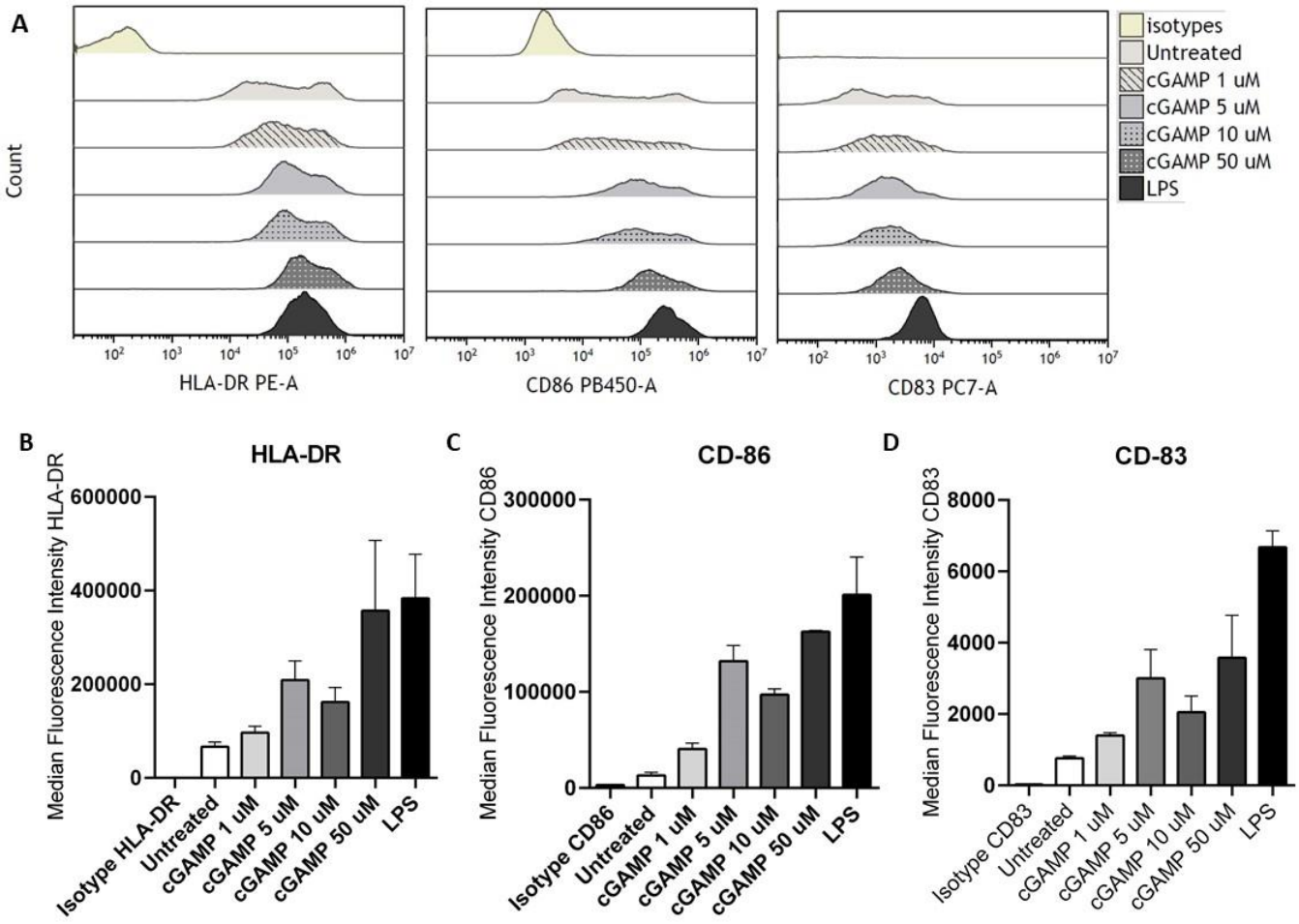

Figure 15. cGAMP induced mcDCs maturation. **A)** Flow cytometry analysis of maturation markers HLA-DR, CD86 and CD83 after dendritic cell stimulation with different concentrations of 2'3'-cGAMP (example of histograms from one experiment) **B), C)** and **D)** Bar charts of median fluorescence intensity. The data is an average from two independent experiments. The error bars present the standard error of the mean of the collected data.

A difference between 1μM and the higher concentrations of 2'3'-cGAMP could be observed in histograms. 1μM of 2'3'-cGAMP did not increase of the expression of maturation markers as much as the rest of the used cGAMP concentrations (figure 15 A)

Similar results from the median fluorescence intensity of three markers could be seen for human cells. The highest peaks are for samples stimulated with 5 and 50μM of 2'3'-cGAMP, which are closer to the level of positive LPS control value than to an untreated sample's value (figure 15 B-D).

Next, human moDCs were stimulated overnight with nystatin in concentrations varying from 7.6U/ml up to 150U/ml alone or in combination with 5μM 2'3'-cGAMP (figure 16).

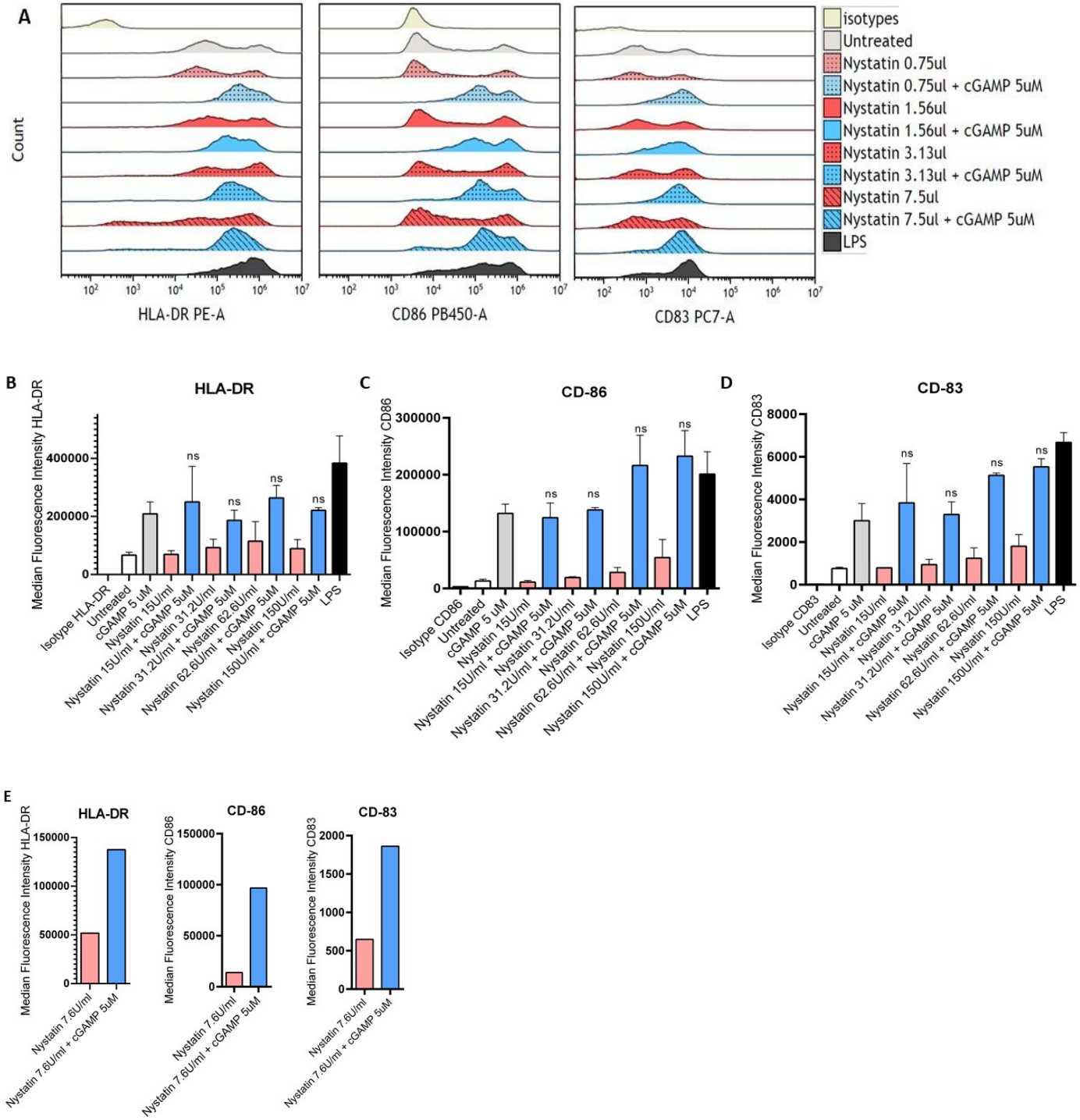

Figure 16. Nystatin and cGAMP effect on moDCs maturation **A)** Flow cytometry analysis of maturation markers HLA-DR, CD86 and CD83 after dendritic cell stimulation with different concentrations nystatin and its combination with 5μM of 2'3'-cGAMP (example of histograms from one experiment). **B), C)** and **D)** Bar charts of median fluorescence intensity. The data is an average from two independent experiments. The error bars present the standard error of the mean of the collected data. **E)** Results from samples called 'Nystatin 7.6U/ml' and 'Nystatin 7.6U/ml + cGAMP 5uM' were collected only from one experiment and statistical analysis was not performed on those samples.

Addition of 5μM of 2'3'-cGAMP to nystatin increased the values of the median fluorescence intensity. However, even if the change is visible there is no significant difference in comparison to stimulation only with 5μM of 2'3'-cGAMP (figure 16). The difference between samples of cells stimulated only with nystatin and with the addition of 2'3'-cGAMP can be observed on histograms (figure 16A). In some cases, the effect of experimental samples (e.g. nystatin 150U/ml + 5μM of 2'3'-cGAMP) on the presence of CD86 maturation marker was higher than for the sample stimulated with LPS (figure 16C).

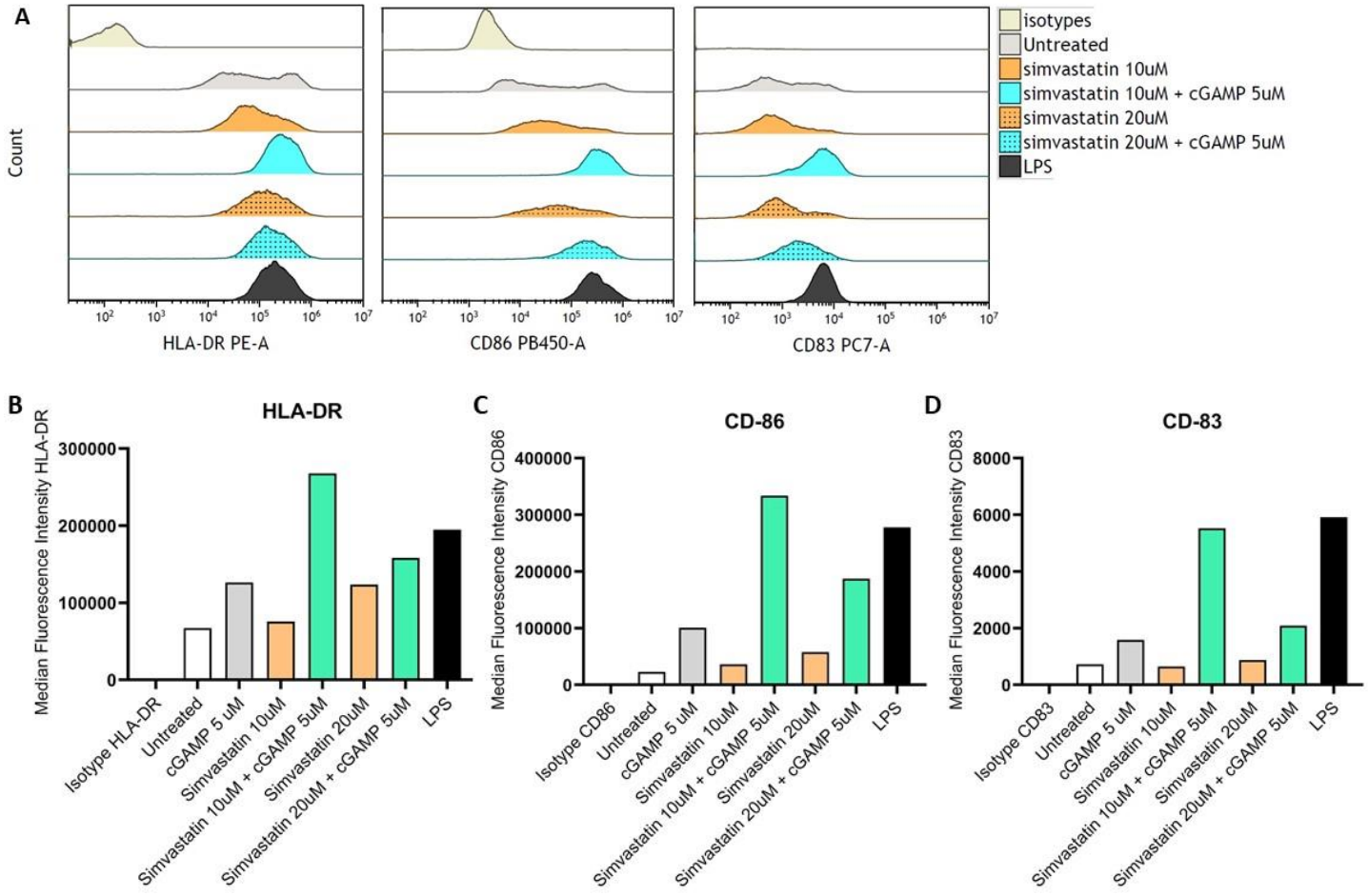

Figure 17. Simvastatin and cGAMP effect on moDCs maturation. **A)** Flow cytometry analysis of maturation markers HLA-DR, CD86 and CD83 after dendritic cell stimulation with different concentrations simvastatin and its combination with 5μM of 2'3'-cGAMP (example of histograms from one experiment). **B), C)** and **D)** Bar charts of median fluorescence intensity. Because the data is collected from one experiment, statistical analysis was not performed.

The results from human DCs treated with simvastatin provide a different outcome in comparison to the results of simvastatin stimulation of murine cells. The highest peak of median fluorescence intensity (HLA-DR and CD86) was for a sample treated with 10μM of simvastatin and 5μM of the 2'3'-cGAMP.

However, because of the lack of data (simvastatin was tested only on one donor), the statistical analysis could not be performed (figure 17).

3.2. cGAMP and nystatin induced type-I IFN production in THP1 cells

3.2.1. Detection of IFN-I in supernatant from THP-1 macrophages cells

An experiment with HEK-Blue™ was performed in order to test if nystatin and 2'3'-cGAMP are able to activate the STING pathway, which leads to IFN-I production. Two types of THP-1 monocytes (WT and knockout of the STING protein) were differentiated into macrophages and stimulated with nystatin and 2'3'-cGAMP in different concentrations for 24 hours. The HEK-Blue cells are designed to allow the detection and measurement of IFN-I e.g. from supernatants of THP-1 cells.

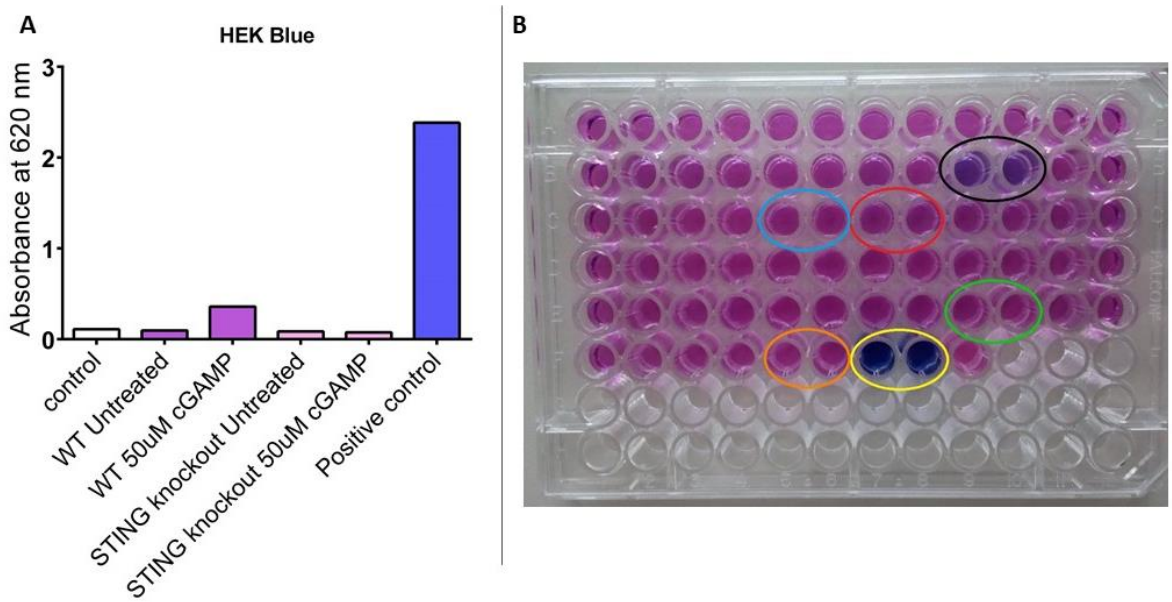

Figure 18. Effect of 2'3'-cGAMP on IFN-I production (HEK/blue™ assay). **A)** Bar chart of spectrophotometric measurement. **B)** picture of the 96 well plate with samples of supernatant from HEK-Blue cells stimulated with: supernatant from THP-1 WT cells stimulated with 50µM of 2'3'-cGAMP (wells in the black circle); supernatant from untreated THP-1 WT (wells in the blue circle); supernatant from THP-1 STING knockout stimulated with 50µM of 2'3'-cGAMP (wells in green circle); supernatant from untreated THP-1 STING knockout (wells in orange circle);positive control (wells in the yellow circle) and control sample without stimulation (wells in the red circle).

Only HEK/blue™ cells with addition of supernatant from THP-1 WT macrophages stimulated with 50µM of 2'3'-cGAMP, showed a visible difference in the assay (figure 18).

To investigate if nystatin could increase the IFN-I production, THP-1 macrophages were stimulated with nystatin (120U/ml) in combination with either 50µM or 5µM of 2'3-'cGAMP (figure 19).

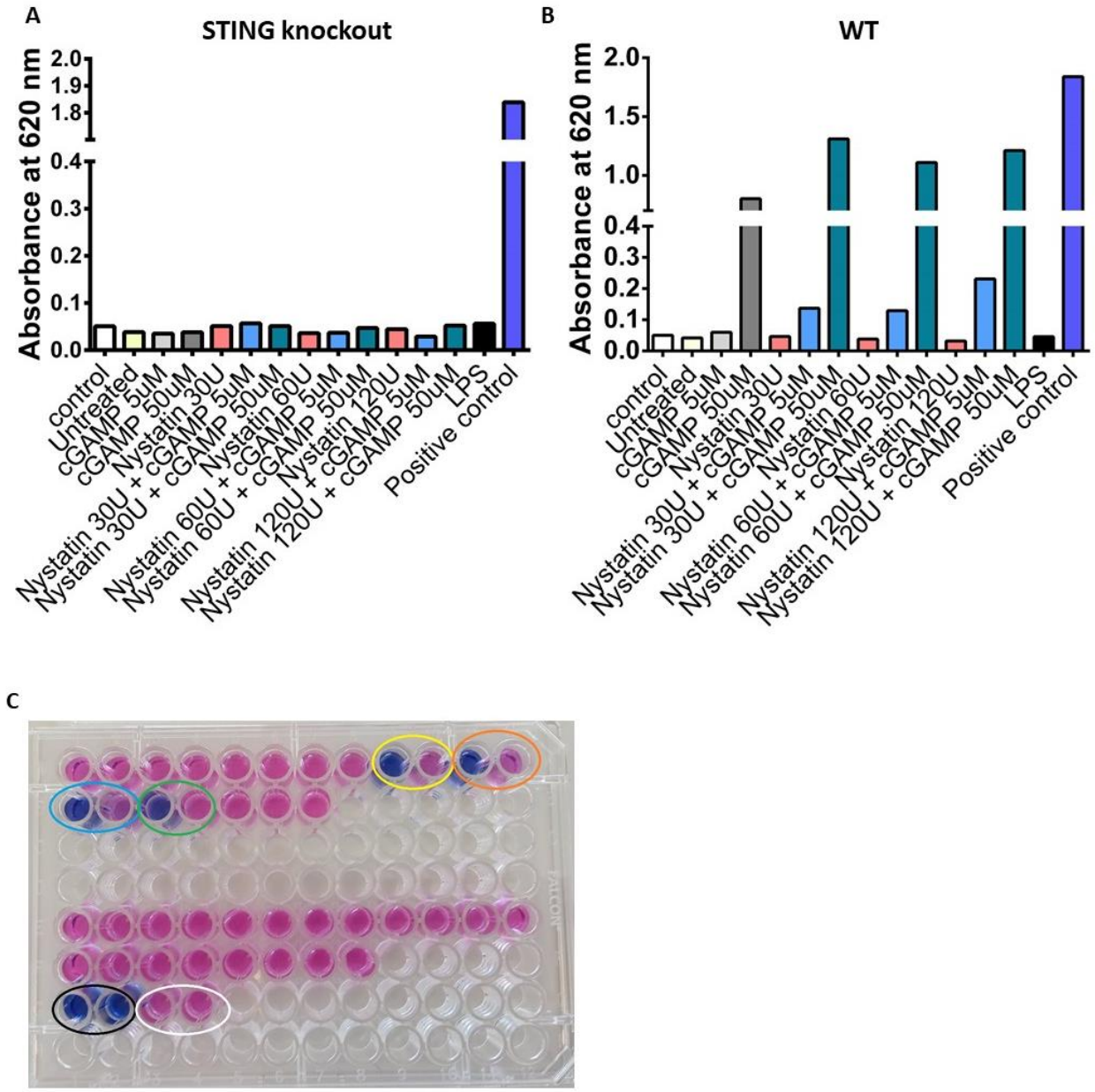

Figure 19. Effect of Nystatin and 2'3'-cGAMP on IFN-I production (HEK/blue™ assay). **A)** and **B)** Bar charts of spectrophotometric measurement from samples of THP-1 STING knockout and THP-1 WT respectively. **C)** picture of the 96 well plate with samples of supernatant from HEK-Blue cells stimulated with: supernatant from THP-1 WT cells stimulated with 30U/ml of nystatin in combination with 5μM and 50μM of 2'3'-cGAMP (wells in the yellow circle); supernatant from THP-1 WT cells stimulated with 60U/ml of nystatin in combination with 50μM and 5μM of 2'3'-cGAMP (wells in the orange circle); supernatant from THP-1 WT cells stimulated with 120U/ml of nystatin in combination with 50μM and 5μM of 2'3'-cGAMP (wells in the blue circle);supernatant from THP-1 WT treated with 50μM and 5μM of 2'3'-cGAMP (wells in the green circle);positive control (wells in the black circle) and control sample without stimulation (wells in the white circle).

Results of absorbance show that every single used concentration of nystatin enhanced activity of 2'3'-cGAMP (50μM) on IFN-I production. From bar charts it can be also observed that IFN-I production was higher within cells stimulated with 5μM of 2'3'-cGAMP combined with nystatin, especially with 120U/ml (figure 19B).

Results for THP-1 macrophages with knockout of the Tmem175 gene (encoding the STING protein) were at similar level as for the unstimulated control sample, confirming the importance of the STING pathway (figure 19A).

4. Discussion

During the experiment in this thesis, two drugs with cholesterol inhibiting properties were tested to investigate if they can increase 2'3'-cGAMP induced activation of the STING pathway.

The endpoint of the STING pathway is the production of IFN-I, which has a variety of immunomodulatory functions like affecting the activity of DCs, leading to their maturation and induction of further expression of IFN-I. This cytokine works as an anti-angiogenic, antiviral and antitumor factor, which has gained an increased interest in the immunotherapy field. However, despite the many pro-inflammatory and antitumor functions, IFN-I can also work in favor of the tumor progression. Under specific conditions, IFN-I can induce production of IL-10, IDO and it is required for maintenance of PD-L1 molecules [67]. Teijaro et al. conducted a study where they blocked IFN-I signaling in mice infected with lymphocytic choriomeningitis virus before and after the establishment of infection. The blockage caused progression of the viral replication when antibody neutralizing IFNAR1 was applied one day before infection. However, when mice received anti-IFNAR1 antibody on the 10^{th} day post-infection it led to the suppression of IL-10 and PD-L1 [67], [68]. It can be stated that not only dosage but also the time of IFN-I injection can play an essential role in the regulation of immune response.

There are two major types of IFN-I, α and β where pDCs are more prone to secrete IFN-α type [69]. The difference between type α and β is their affinity towards IFNAR1 and 2. IFN-β bind to its receptor with a higher affinity and the binding is more stable [67]. IFN-β is produced by many cell types, among them are endothelial cells often present in the TME [39].This observation might be crucial during *in vivo* studies, where drug affects more than one cell type. Nonetheless, this project was mainly focused on DCs and their ability to produce IFN-I signaling under STING stimulation.

To activate the STING pathway 2'3'-cGAMP was used. 2'3'-cGAMP is a cyclic-dinucleotide and ligand of the STING protein. It was confirmed, by several studies that the exogenous cGAMP molecules are able to activate the pathway, which results in IFN-I production [52]. The cGAMP and other cyclic-dinucleotides in combination with checkpoints inhibitors are proposed as a cancer treatment option [70]. The cGAMP molecules have a short lifetime, however, there were implicated some modification to the structure that can prolong half lifetime e.g. Lingyin Li et al. modified 2'3'-cGAMP by addition of the phosphothioate linkages 2′3′-cG^{S}A^{S}MP [71].

Maturation of DCs can be observed by measuring the level of specific maturation markers, such as CD86, CD83 and MHC-II/HLA-DR. Flow cytometry was used to measure the expression level of maturation markers on murine and human DCs stimulated with different concentrations of cholesterol inhibitors and 2'3'-cGAMP.

During the experiment, murine DCs were collected from BALB/c and C57BL/6 mice. For DCs collected from BALB/c mice the highest ratio of mature cells was found when cells were stimulated with 50μM of 2'3'-cGAMP (MHC-II and CD86 marker). Those expression values were similar to values from LPS stimulation, which was used as a positive control, with the purpose of inducing DCs maturation [72].

The median fluorescence of MHC-II marker is higher for samples treated with 5μM 2'3'-cGAMP and nystatin than when stimulated only with 5μM 2'3'-cGAMP. However, the difference between results was not statistically significant.

According to Toshikazu Shiraha et al. BALB/c mice are very poor IFN-I producers, while one of the best strain of mouse in IFNs production is C57BL/6 [73]. Due to the fact, that IFN-I plays a role in inducing DCs maturation after activation of the STING pathway it was decided to conduct an experiment on cells collected from C57BL/6 mice. Results from flow cytometry of DCs collected from C57BL/6 mice shows that any concentration of 2'3'-cGAMP influence the maturation of cells. When 2'3'-cGAMP was combined with nystatin the MHC-II maturation marker was raised but the difference was not significant. In contrast, results from flow cytometry analysis of CD86 maturation marker showed a clearer outcome. For DCs from both mice strains, a combination of nystatin with 5μM 2'3'-cGAMP resulted in higher peaks than stimulation with 5μM 2'3'-cGAMP only and the difference was statistically significant.

Based on this it could be stated that CD86 is a more efficient marker because results from this marker showed a clearer image. MHC-II and CD86 are some of the most sensitive maturation markers and appear on the surface of mature DCs on the highest level among other markers [74].

During intracellular transport of MHC-II-Ii complexes, first, a transit through the Golgi apparatus occurs, which is associated with lipid rafts. It is estimated that lipid rafts are taking part in the transport of around 60% of newly synthesized MHC-II to the cell surface and occur during protein processing. Lipid rafts' molecule composition contains cholesterol, sphingomyelin, and gangliosides [75]. Cholesterol inhibition within DCs could impact the transport of MHC-II molecules and by that make MHC-II an inaccurate maturation marker during these experiments.

Since the human and murine immune system differs in several aspects, future implementation of nystatin and simvastatin for use in cancer therapy on humans will require a test on human DCs. To investigate if there is compliance between human and murine DC maturation cholesterols inhibitors combined with 2'3'-cGAMP were tested on human DCs differentiated from monocytes.

For human DCs the panel of maturation markers was increased by an anti-CD83 antibody.

When stimulated with pure 2'3'-cGAMP, the highest expression was for 50μM where the expression values were comparable to the effect of LPS. Furthermore, it could be seen that 5μM of 2'3'-cGAMP works relatively good on its own and particularly when combined with nystatin.

Although the maturation markers panel for the experiments on human DCs was enlarged by the inclusion of an anti-CD83 antibody the addition of another antibody indicating maturation of DCs such as anti-CD40 is suggested for future studies. Furthermore, the MHC-II marker may not be an optimal maturation marker in experiments where cholesterol inhibitors are tested.

According to Ernest C. Borden et al. nystatin leads to increased interferon production due to the macrocyclic lactone ring. Their experiment included stimulation of murine fibroblast cells (L929) with poly I:C and polyene macrolides such as nystatin. They concluded that the addition of polyene macrolides to cells stimulated with poly I:C, enhanced interferon production from 10 to 100 times. They tested drugs with macrocyclic lactone ring like amphotericin, amphotericin methyl ester, nystatin, filipin and retinol, which is a non-macrolide polyene. The most effective drug for increasing interferon production was amphotericin, which is water-soluble. Non-macrolide polyene was ineffective in enhancing interferon production. Concentrations of nystatin used during that study were from 10 up to 1000μg/ml in combination with 50μg/ml of poly I:C. However, the working concentration of nystatin was obtained between 70-500μg/ml and the highest IFN-I production was established after stimulation with 500μg/ml of nystatin. These results brought authors to the conclusion that the macrolide ring as a part of the chemical structure is essential in enhancing interferon synthesis [59]. The nystatin solution used in my experiments was made in DPBS. Nystatin formed crystal structures, so it was hard to adjust the required concentration. However, there is a modified version of nystatin available on the market, which can be dissolved in water-based liquids. As it was mentioned above, Ernest C. Borden et al. suggest that water-soluble macrolide drugs work better in enhancing interferon production [59]. To see whether water solubility has an impact it would be relevant to test both versions of the drug.

The concentration of nystatin used during this project was given in units. According to the WHO one unit of nystatin is corresponding to 0.000333 mg of the international standard [76]. During my studies, the concentration of nystatin, which was the most effective in increasing DC maturation was between 30-60 U/ml for murine cells and 60-150 U/ml for human cells. Nystatin in the concentration of 150U/ml is corresponding to 50 μg/ml. It was the highest used concentration during my experiment, and it is lower than drug's working concentration in Ernest C. Borden's study.

According to Reeta T. Mehta et al. free nystatin applied intravenously is toxic for mice in a concentration above 4 mg/kg of body weight. To lower the toxicity of the drug and increase

effectiveness they encapsulated nystatin in liposomes. After encapsulation toxicity was lower the MTD was 16 mg/kg of the drug in one intravenous injection and around 80 mg/kg in multiple injections [77]. Another study conducted by R. Semis, et al. came up with a similar concept of encapsulating nystatin in an intralipid formulation [78]. Both experiments tested nystatin to treat fungal infections, however, the concept of encapsulation could be applied in immunotherapy research. On the other hand, nystatin could be applied in topological treatment in case of skin cancers such as melanoma.

As Ernest C. Borden et al. suggest high concentration of nystatin perforates cell membrane and by that it could increase the permeability of poly I:C through cell membrane [59]. This explanation could also be applied to external 2'3'-cGAMP administration, due to the fact, that 2'3'-cGAMP is binding to the STING protein, which is located inside the cell, on the ER membrane. On the other hand, the concentration of nystatin used during this project is much lower than in Ernest C. Borden study. Moreover, viability of cells treated with nystatin is high (figure s1). Therefore, the cell membrane should not be damaged and there has to be another mechanism that could explain the way of nystatin action. It is worth to mention that due to negatively charged cell membrane cGAMP cannot passively cross the membrane. Moreover, SLC19A1 is a newly discovered receptor, which imports cGAMP inside the cell cytoplasm [79]. Interestingly, change of the density of cholesterol has impact on changing surface charge [80]. There is also a possibility that nystatin binding to cholesterol molecules within the cell membrane loosens the tight structure of phospholipid head groups and make possible for cGAMP to cross the cell membrane. A study conducted by Autumn G. York et al. find that cholesterol biosynthesis and expression of interferon I genes are co-regulated. According to that study, IFN-I signaling shifts cholesterol metabolism in order to inhibit biosynthesis and increase cholesterol efflux from the environment. They theorize that depriving the ER membrane of cholesterol, changes the binding between the ER membrane and the STING protein, promoting the activation of STING and facilitating STING/TBK1 binding [62].

The second tdrug tested here was simvastatin, which works as an inhibitor of HMG-CoA reductase. This enzyme plays a crucial role in cholesterol biosynthesis. The analysis of murine DCs showed that stimulation with simvastatin brought a similar outcome as the untreated sample, and results from samples treated by simvastatin combined with 5μM of 2'3'-cGAMP are similar to cells treated with 5μM of 2'3'-cGAMP alone. However, human DCs stimulated with 10μM of simvastatin combined with 5μM of 2'3'-cGAMP demonstrated highly increased expression compared to cells treated only with 5μM of 2'3'-cGAMP. Nonetheless, this cholesterol inhibitor was tested on cells from only one human donor and it must be repeated to fully verify the simvastatin effect on human DCs.

In theory, simvastatin which works as an inhibitor of cholesterol biosynthesis was considered as an ideal candidate to confirm assumption from Autumn G. York et al. study. Nonetheless, by taking into account the results from this study, simvastatin did not increase the maturation of DCs.

The low effect of simvastatin could be caused by too short stimulation time. Optionally, an experiment where simvastatin was given 24, 48 and 72 hours before samples collection could have been conducted.

To confirm that cholesterol inhibitor drugs in combination with 2'3'-cGAMP influences IFN-I production the production of IFN-I was analyzed using a HEK/Blue™ cell reporter assay. For this assay, THP-1 monocytes and macrophages were used. THP-1 derived macrophages are considered to be very good IFN-I producers after activation of the STING pathway [81]. The laboratory of immunology at Aalborg University had a modified THP-1 cell line with the STING knockout, which could be used to test the dependency on STING signaling pathway.

The HEK/Blue™ cell assay did not bring positive outcome on THP-1 monocyte cells. According to Hayes et al. monocytes are not preferable cell type to produce IFN-I and are able to do it only under presence of GM-CSF or IFN-γ in the culture medium [82]. With this in mind, THP-1 monocytes were differentiated into macrophages. After one experiment on THP-1 macrophages, the only difference was seen in the wells with THP-1 WT macrophages stimulated with 50μM of 2'3'-cGAMP. Combination of nystatin with 2'3'-cGAMP resulted in higher IFN-I production in comparison to cells stimulated only with 2'3'-cGAMP. Moreover, THP-1 STING knockout cells failed to produce IFN-I after stimulation with 50μM of 2'3'-cGAMP, which confirms that the HEK/Blue™ assay can be used to detect STING-specific macrophage activation by extracellular STING agonists. It would be interesting to repeat this assay and block the SLC19A1 receptor. This could give an answer whether nystatin enable passive transport of 2'3'-cGAMP molecule through cell membrane.

During my experiments, it was observed that the effect of 2'3'-cGAMP and cholesterol inhibitors on DC maturation differs even among individuals within the same species. Activation of the STING pathway and its efficiency might be dependent on genetic or biological factors. Individuals that better react to 2'3'-cGAMP treatment might be carriers of gene polymorphisms. To fully see whether there is a genetic variation among genes related to the STING pathway gene sequencing should be performed and comparison of sequence between good and bad responders could be applied. It might be crucial to apply it before any clinical attempts. It is worth to mention that there are already known several polymorphisms within the TMEM173 gene, which is the coding sequence for the STING protein. Two discovered variants HAQ and H232 are considered as a TMEM173 loss of function alleles [83].

This project examined two cholesterol inhibitors, which may have potential application in combination immuno-therapeutics. However, both of the drugs work in a different manner.

As it was stated previously, nystatin in higher concentration creates barrel-like complexes and by that perforates cell membrane. On the other hand, simvastatin blocks HMG-CoA-reductase enzyme. Both drugs target cholesterol, which is an essential component of the cell membrane. With this in mind drugs, which target and blocks cholesterol molecules or its synthesis in higher dosage will be toxic at the cellular and organismal level.

New drug development is time and costs consuming. Moreover, a new substance must undergo years of testing from clinical trials to safety testing before it can be brought on the market. Many researchers are looking for effective oncological drugs among already existing medicaments. Some cholesterol inhibitors e.g. nystatin and simvastatin have already been approved by the FDA as a therapeutic against fungal infections and as a cholesterol level lowering drug, respectively. The major advantage of testing nystatin and simvastatin for cancer treatment would be an easier procedure for introducing them on the market.

4.1. Conclusion

From the results presented in this project, it can be concluded that nystatin in combination with cGAMP can increase maturation of DCs. Although more studies have to be conducted to fully understand the mechanism of nystatin action. On the other hand, simvastatin did not work as well as nystatin and even decreased activity of cGAMP in cell maturation. It must be mentioned that collected data of cells stimulated with simvastatin was limited and it should be repeated to confirm this statement.

HEK/Blue™ assay provided results in which nystatin can enhance the activity of STING agonist in IFN-I production. However, this assay should be repeated to fully confirm this observation.

Due to the shortage of time frame of the project, some of the planned experiments had to be cancelled like ELISA assay and *in vivo* experiments on mice. However, it is still recommended do perform ELISA on supernatants from murine DCs stimulated to measure secreted IFN-I and IL-12 and *in vivo* experiment of mice with subcutaneous tumors treated with injections of nystatin directly to tumor tissues.

Nonetheless, there is a potential of cholesterol inhibitors and the cGAMP to be used in order of activation the STING pathway and future application as a combinatory therapy with other cancer therapeutic approaches such as checkpoints inhibitors.

5. References

[1] F. Bray, J. Ferlay, I. Soerjomataram, R. L. Siegel, L. A. Torre, and A. Jemal, “Global cancer statistics 2018: GLOBOCAN estimates of incidence and mortality worldwide for 36 cancers in 185 countries,” *CA. Cancer J. Clin.*, vol. 68, no. 6, pp. 394–424, 2018.

[2] L. Hood and S. H. Friend, “Predictive, personalized, preventive, participatory (P4) cancer medicine,” *Nat. Rev. Clin. Oncol.*, vol. 8, no. 3, pp. 184–187, 2011.

[3] Max Roser and Hannah Ritchie, “Cancer,” 2019. [Online]. Available: https://ourworldindata.org/cancer#cancer-deaths-by-age. [Accessed: 25-May-2020].

[4] Cancer Society of Finland, “Cancer after the age of 75.” [Online]. Available: https://www.cancersociety.fi/publications/reports/cancer-in-finland-2016/cancers-after-the-age-of-75/. [Accessed: 25-May-2020].

[5] A. Durgeau, Y. Virk, S. Corgnac, and F. Mami-Chouaib, “Recent advances in targeting CD8 T-cell immunity for more effective cancer immunotherapy,” *Front. Immunol.*, vol. 9, no. JAN, 2018.

[6] C. E. Clark and R. H. Vonderheide, “Getting to the surface: A link between tumor antigen discovery and natural presentation of peptide-MHC complexes,” *Clin. Cancer Res.*, vol. 11, no. 15, pp. 5333–5336, 2005.

[7] J. Banchereau and A. K. Palucka, “Dendritic cells as therapeutic vaccines against cancer,” *Nat. Rev. Immunol.*, vol. 5, no. 4, pp. 296–306, 2005.

[8] G. P. Dunn, L. J. Old, and R. D. Schreiber, “The immunobiology of cancer immunosurveillance and immunoediting,” *Immunity*, vol. 21, no. 2, pp. 137–148, 2004.

[9] R. D. Schreiber, L. J. Old, and M. J. Smyth, “Cancer immunoediting: Integrating immunity’s roles in cancer suppression and promotion,” *Science (80-.).*, vol. 331, no. 6024, pp. 1565–1570, 2011.

[10] M. Friedrich *et al.*, “Tumor-induced escape mechanisms and their association with resistance to checkpoint inhibitor therapy,” *Cancer Immunol. Immunother.*, vol. 68, no. 10, pp. 1689–1700, 2019.

[11] M. Wang *et al.*, “Role of tumor microenvironment in tumorigenesis,” *J. Cancer*, vol. 8, no. 5, pp. 761–773, 2017.

[12] Y. Yuan, Y. C. Jiang, C. K. Sun, and Q. M. Chen, “Role of the tumor microenvironment in tumor progression and the clinical applications (Review),” *Oncol. Rep.*, vol. 35, no. 5, pp. 2499–2515, 2016.

[13] H. Nishikawa and S. Sakaguchi, “Regulatory T cells in tumor immunity,” *Int. J. Cancer*, vol. 127, no. 4, pp. 759–767, 2010.

[14] P. Carmeliet, “VEGF as a key mediator of angiogenesis in cancer,” *Oncology*, vol. 69, no. SUPPL. 3, pp. 4–10, 2005.

[15] WHO, “Lymphatic Filariasis: Practical Entomology - A Handbook for National Elimination Programmes,” *WHO Libr. Cat. Data*, vol. 16, no. 4, pp. 1--107, 2013.

[16] F. C. Chou, H. Y. Chen, C. C. Kuo, and H. K. Sytwu, “Role of galectins in tumors and in clinical immunotherapy,” *Int. J. Mol. Sci.*, vol. 19, no. 2, 2018.

[17] F. Garrido, F. Ruiz-Cabello, and N. Aptsiauri, “Rejection versus escape: the tumor MHC dilemma,” *Cancer Immunol. Immunother.*, vol. 66, no. 2, pp. 259–271, 2017.

[18] M. W. L. Teng, J. Galon, W. H. Fridman, and M. J. Smyth, “From mice to humans: Developments in cancer immunoediting,” *J. Clin. Invest.*, vol. 125, no. 9, pp. 3338–3346, 2015.

[19] A. Gardner and B. Ruffell, “Dendritic Cells and Cancer Immunity,” *Trends Immunol.*, vol. 37, no. 12, pp. 855–865, 2016.

[20] J. W. Rhodes, O. Tong, A. N. Harman, and S. G. Turville, “Human dendritic cell subsets, ontogeny, and impact on HIV infection,” *Front. Immunol.*, vol. 10, no. MAY, 2019.

[21] C. Macri, E. S. Pang, T. Patton, and M. O’Keeffe, “Dendritic cell subsets,” *Semin. Cell Dev. Biol.*, vol. 84, pp. 11–21, 2018.

[22] R. Noubade, S. Majri-Morrison, and K. V. Tarbell, “Beyond CDC1: Emerging roles of DC crosstalk in cancer immunity,” *Front. Immunol.*, vol. 10, no. MAY, pp. 1–13, 2019.

[23] M. Collin and V. Bigley, “Human dendritic cell subsets: an update,” *Immunology*, vol. 154, no. 1, pp. 3–20, 2018.

[24] T. A. Patente, M. P. Pinho, A. A. Oliveira, G. C. M. Evangelista, P. C. Bergami-Santos, and J. A. M. Barbuto, “Human dendritic cells: Their heterogeneity and clinical application potential in cancer immunotherapy,” *Front. Immunol.*, vol. 10, no. JAN, pp. 1–18, 2019.

[25] M. B. Fuertes, S. R. Woo, B. Burnett, Y. X. Fu, and T. F. Gajewski, “Type I interferon response and innate immune sensing of cancer,” *Trends Immunol.*, vol. 34, no. 2, pp. 67–73, 2013.

[26] A. Lin, A. Schildknecht, L. T. Nguyen, and P. S. Ohashi, “Dendritic cells integrate signals from the tumor microenvironment to modulate immunity and tumor growth,” *Immunol. Lett.*, vol. 127, no. 2, pp. 77–84, 2010.

[27] M. Tang, J. Diao, and M. S. Cattral, “Molecular mechanisms involved in dendritic cell dysfunction in cancer,” *Cell. Mol. Life Sci.*, vol. 74, no. 5, pp. 761–776, 2017.

[28] S. Bohnenkamp, V. LeBaron, and L. H. Yoder, “The medical-surgical nurse’s guide to ovarian cancer: Part II.,” *Medsurg Nurs.*, vol. 16, no. 5, 2007.

[29] N. Vutakuri, “Curcumin - Breast Cancer Therapeutic Agent to Replace Allopathic Treatments with Extensive Side Effects,” *J. Young Investig.*, vol. 35, no. 2, pp. 38–44, 2018.

[30] National Cancer Institute, “Radiation Therapy to Treat Cancer,” 2019. [Online]. Available: https://www.cancer.gov/about-cancer/treatment/types/radiation-therapy. [Accessed: 25-May-2020].

[31] P. Dobosz and T. Dzieciątkowski, “The Intriguing History of Cancer Immunotherapy,” *Front. Immunol.*, vol. 10, no. December, 2019.

[32] N. E. Papaioannou, O. V. Beniata, P. Vitsos, O. Tsitsilonis, and P. Samara, “Harnessing the immune system to improve cancer therapy,” *Ann. Transl. Med.*, vol. 4, no. 14, 2016.

[33] E. I. Buchbinder and A. Desai, “CTLA-4 and PD-1 pathways similarities, differences, and implications of their inhibition,” *Am. J. Clin. Oncol. Cancer Clin. Trials*, vol. 39, no. 1, pp. 98–106, 2016.

[34] H. T. Lee, S. H. Lee, and Y. S. Heo, “Molecular interactions of antibody drugs targeting PD-1, PD-L1, and CTLA-4 in immuno-oncology,” *Molecules*, vol. 24, no. 6, pp. 1–16, 2019.

[35] D. V Chan *et al.*, “proliferation,” vol. 15, no. 1, pp. 25–32, 2015.

[36] K. D. McCoy and G. Le Gros, “The role of CTLA-4 in the regulation of T cell immune responses,” *Immunol. Cell Biol.*, vol. 77, no. 1, pp. 1–10, 1999.

[37] Y. Iwai, J. Hamanishi, K. Chamoto, and T. Honjo, “Cancer immunotherapies targeting the PD-1 signaling pathway,” *J. Biomed. Sci.*, vol. 24, no. 1, pp. 1–11, 2017.

[38] S. Di Franco, A. Turdo, M. Todaro, and G. Stassi, “Role of Type I and II interferons in colorectal cancer and melanoma,” *Front. Immunol.*, vol. 8, no. JUL, 2017.

[39] O. Demaria *et al.*, “STING activation of tumor endothelial cells initiates spontaneous and therapeutic antitumor immunity,” *Proc. Natl. Acad. Sci. U. S. A.*, vol. 112, no. 50, pp. 15408–15413, 2015.

[40] H. O. Sintim, C. G. Mikek, M. Wang, and M. A. Sooreshjani, “Interrupting cyclic dinucleotide-cGAS–STING axis with small molecules,” *Medchemcomm*, vol. 10, no. 12, pp. 1999–2023, 2019.

[41] F. Braza, S. Brouard, S. Chadban, and D. R. Goldstein, “Role of TLRs and DAMPs in allograft inflammation and transplant outcomes,” *Nat. Rev. Nephrol.*, vol. 12, no. 5, pp. 281–290, 2016.

[42] R. S. Mahla, M. C. Reddy, D. Vijaya Raghava Prasad, and H. Kumar, “Sweeten PAMPs: Role of sugar complexed PAMPs in innate immunity and vaccine biology,” *Front. Immunol.*, vol. 4, no. SEP, pp. 1–16, 2013.

[43] M. Smith *et al.*, “Trial Watch: Toll-like receptor agonists in cancer immunotherapy,” *Oncoimmunology*, vol. 7, no. 12, pp. 1–15, 2018.

[44] M. Matsumoto and T. Seya, “TLR3: Interferon induction by double-stranded RNA including poly(I:C),” *Adv. Drug Deliv. Rev.*, vol. 60, no. 7, pp. 805–812, 2008.

[45] A. Basit, M. G. Cho, E. Y. Kim, D. Kwon, S. J. Kang, and J. H. Lee, “The cGAS/STING/TBK1/IRF3 innate immunity pathway maintains chromosomal stability through regulation of p21 levels,” *Exp. Mol. Med.*, 2020.

[46] D. Gao *et al.*, “Cyclic GMP-AMP Synthase Is an,” vol. 1375, no. July, pp. 903–907, 2013.

[47] J. Tao, X. Zhou, and Z. Jiang, “cGAS-cGAMP-STING: The three musketeers of cytosolic DNA sensing and signaling,” *IUBMB Life*, vol. 68, no. 11, pp. 858–870, 2016.

[48] Q. Chen, L. Sun, and Z. J. Chen, “Regulation and function of the cGAS-STING pathway of cytosolic DNA sensing,” *Nat. Immunol.*, vol. 17, no. 10, pp. 1142–1149, 2016.

[49] L. Corrales *et al.*, “Direct Activation of STING in the Tumor Microenvironment Leads to Potent and Systemic Tumor Regression and Immunity,” *Cell Rep.*, vol. 11, no. 7, pp. 1018–1030, 2015.

[50] B. A. Flood, E. F. Higgs, S. Li, J. J. Luke, and T. F. Gajewski, “STING pathway agonism as a cancer therapeutic,” *Immunol. Rev.*, vol. 290, no. 1, pp. 24–38, 2019.

[51] H. Liang *et al.*, “Host STING-dependent MDSC mobilization drives extrinsic radiation resistance,” *Nat. Commun.*, vol. 8, no. 1, pp. 1–10, 2017.

[52] L. Deng *et al.*, “STING-dependent cytosolic DNA sensing promotes radiation-induced type I interferon-dependent antitumor immunity in immunogenic tumors,” *Immunity*, vol. 41, no. 5, pp. 843–852, 2014.

[53] C. for D. E. and Research, “Application number 64142.” p. Application number 64142, 1998.

[54] A. G. Dos Santos *et al.*, “The molecular mechanism of Nystatin action is dependent on the membrane biophysical properties and lipid composition,” *Phys. Chem. Chem. Phys.*, vol. 19, no. 44, pp. 30078–30088, 2017.

[55] NHS, “Simvastatin.” [Online]. Available: https://www.nhs.uk/medicines/simvastatin. [Accessed: 25-May-2020].

[56] O. T. C. K. M. Cassagnol., “Simvastatin,” 2020.

[57] N. C. for B. I. P. Database., “Nystatin chemical structure.” [Online]. Available: https://pubchem.ncbi.nlm.nih.gov/compound/Nilstat. [Accessed: 25-May-2020].

[58] N. C. for B. I. P. Database., “Simvastatin.” [Online]. Available: https://pubchem.ncbi.nlm.nih.gov/compound/Simvastatin. [Accessed: 25-May-2020].

[59] E. C. Borden, B. W. Booth, and P. H. Leonhardt, “Mechanistic studies of polyene enhancement of interferon production by polyriboinosinic-polyribocytidylic acid,” *Antimicrob. Agents Chemother.*, vol. 13, no. 2, pp. 159–164, 1978.

[60] A. C. Theos *et al.*, “Functions of adaptor protein (AP)-3 and AP-1 in tyrosinase sorting from endosomes to melanosomes,” *Mol. Biol. Cell*, vol. 16, no. November, pp. 5356–

5372, 2005.

[61] N. Dobbs, N. Burnaevskiy, D. Chen, V. K. Gonugunta, N. M. Alto, and N. Yan, “STING activation by translocation from the ER is associated with infection and autoinflammatory disease,” *Cell Host Microbe*, vol. 18, no. 2, pp. 157–168, 2015.

[62] A. G. York *et al.*, “Limiting Cholesterol Biosynthetic Flux Spontaneously Engages Type i IFN Signaling,” *Cell*, vol. 163, no. 7, pp. 1716–1729, 2015.

[63] ATCC, “THP-1 (ATCC® TIB-202™).” [Online]. Available: https://www.lgcstandards-atcc.org/en/Products/All/TIB-202.aspx. [Accessed: 25-May-2020].

[64] InvivoGene, “HEK-Blue™ IFN-α/β Cells.” [Online]. Available: https://www.invivogen.com/hek-blue-ifn-ab. [Accessed: 25-May-2020].

[65] InvivoGene, “QUANTI-BLUE™.” [Online]. Available: https://www.invivogen.com/quanti-blue. [Accessed: 25-May-2020].

[66] C. Ritchie, A. F. Cordova, G. T. Hess, M. C. Bassik, and L. Li, “SLC19A1 Is an Importer of the Immunotransmitter cGAMP,” *Mol. Cell*, vol. 75, no. 2, pp. 372-381.e5, 2019.

[67] R. F. V. Medrano, A. Hunger, S. A. Mendonça, J. A. M. Barbuto, and B. E. Strauss, *Immunomodulatory and antitumor effects of type I interferons and their application in cancer therapy*, vol. 8, no. 41. 2017.

[68] J. R. Teijaro *et al.*, “NIH Public Access,” vol. 340, no. 6129, pp. 207–211, 2013.

[69] S. Ali, R. Mann-Nüttel, A. Schulze, L. Richter, J. Alferink, and S. Scheu, “Sources of type I interferons in infectious immunity: Plasmacytoid dendritic cells not always in the driver’s seat,” *Front. Immunol.*, vol. 10, no. APR, 2019.

[70] T. Su, Y. Zhang, K. Valerie, X. Y. Wang, S. Lin, and G. Zhu, “STING activation in cancer immunotherapy,” *Theranostics*, vol. 9, no. 25, pp. 7759–7771, 2019.

[71] L. Li *et al.*, “Hydrolysis of 2’3’-cGAMP by ENPP1 and design of nonhydrolyzable analogs,” *Nat. Chem. Biol.*, vol. 10, no. 12, pp. 1043–1048, 2014.

[72] R&D Systems, “Dendritic Cell Maturation,” 2002. [Online]. Available: https://www.rndsystems.com/resources/articles/dendritic-cell-maturation. [Accessed: 25-May-2020].

[73] T. Shirahata, A. Mori, H. Ishikawa, and H. Goto, “Strain Differences of Interferon-Generating and Resistance in Toxoplasma-Infected Capacity Mice Akiko MORI , 1 and Hitoshi GOTOI of Veterinary Microbiology , and 2 Veterinary Hospital , Obihiro of Agriculture and Veterinary Medicine , (Accepted for publi,” *Microbiol. Immunol.*, vol. 30, no. 12, pp. 1307–1316, 1986.

[74] M. Dauer *et al.*, “Mature Dendritic Cells Derived from Human Monocytes Within 48 Hours: A Novel Strategy for Dendritic Cell Differentiation from Blood Precursors,” *J. Immunol.*, vol. 170, no. 8, pp. 4069–4076, 2003.

[75] H. A. Anderson and P. A. Roche, “MHC class II association with lipid rafts on the antigen presenting cell surface,” *Biochim. Biophys. Acta - Mol. Cell Res.*, vol. 1853, no. 4, pp. 775–780, 2015.

[76] J. W. LIGHTBOWN, M. KOGUT, and K. UEMURA, “the International Standard for Nystatin.,” *Bull. World Health Organ.*, vol. 29, pp. 87–94, 1963.

[77] R. T. Mehta, R. L. Hopfer, T. McQueen, R. L. Juliano, and G. Lopez-Berestein, “Toxicity and therapeutic effects in mice of liposome-encapsulated nystatin for systemic fungal infections,” *Antimicrob. Agents Chemother.*, vol. 31, no. 12, pp. 1901–1903, 1987.

[78] R. Semis, S. Mendlovic, I. Polacheck, and E. Segal, “Activity of an Intralipid formulation of nystatin in murine systemic candidiasis,” *Int. J. Antimicrob. Agents*, vol. 38, no. 4, pp. 336–340, 2011.

[79] J. A. Carozza *et al.*, “2’3’-cGAMP is an immunotransmitter produced by cancer cells and regulated by ENPP1,” *bioRxiv*, p. 539312, 2019.

[80] A. Magarkar *et al.*, “Cholesterol level affects surface charge of lipid membranes in saline solution,” *Sci. Rep.*, vol. 4, pp. 1–5, 2014.

[81] F. Ma *et al.*, “Positive Feedback Regulation of Type I IFN Production by the IFN-Inducible DNA Sensor cGAS,” *J. Immunol.*, vol. 194, no. 4, pp. 1545–1554, 2015.

[82] M. P. H. J. C. E. T. L. G. K. C. Zoon, “Requirements for Priming for Lipopolysaccharide-Induced Production,” 1991.

[83] S. Patel and L. Jin, “TMEM173 variants and potential importance to human biology and disease,” *Genes Immun.*, vol. 20, no. 1, pp. 82–89, 2019.

6. Supplemental figures

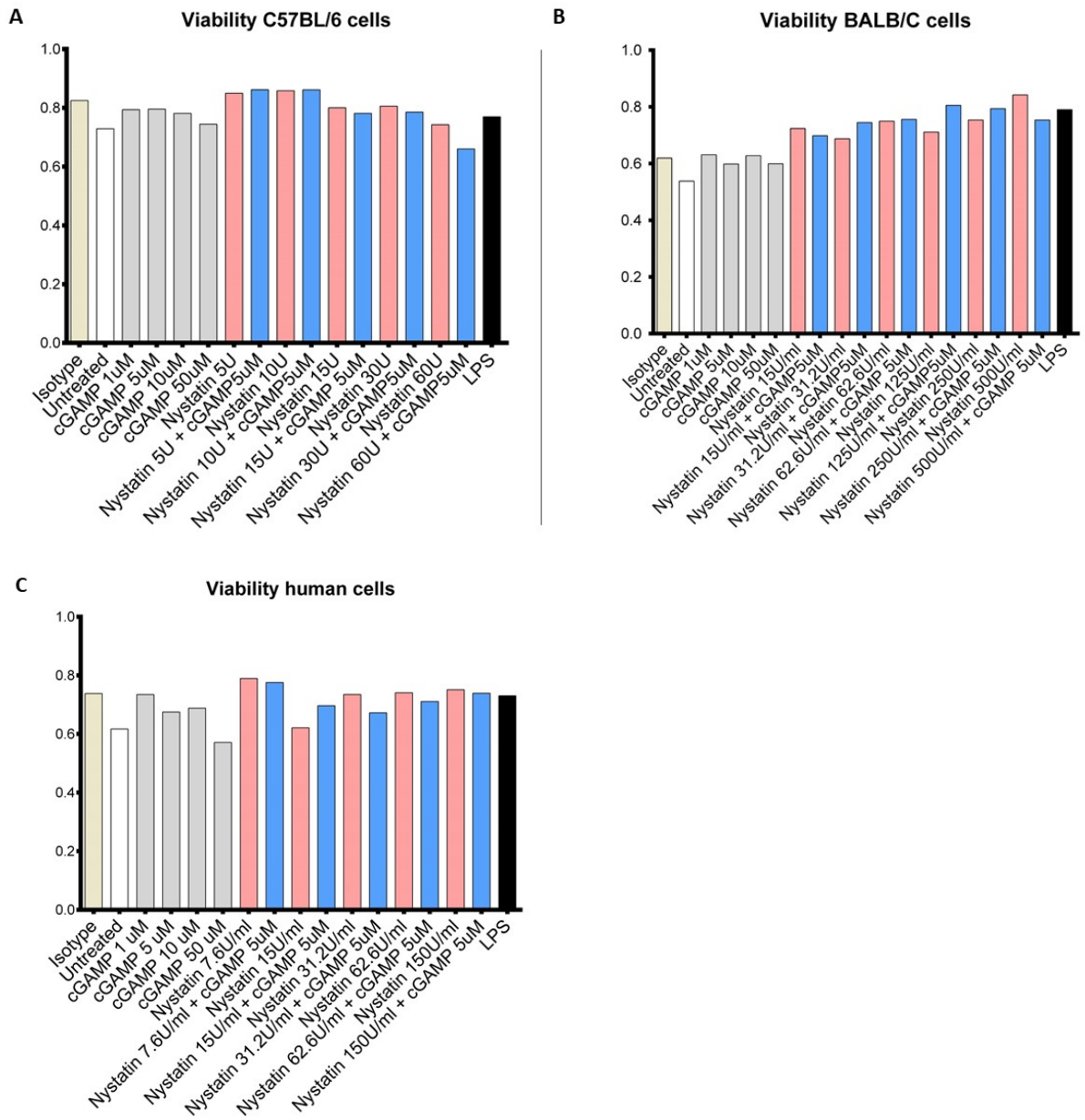

Figure s1. Bar charts of dendritic cell viability after stimulation with nystatin and 2'3'-cGAMP **A)** BMDCs from C57BL/6 strain **B)** BMDCs from BALB/c strain **C)** human moDCs

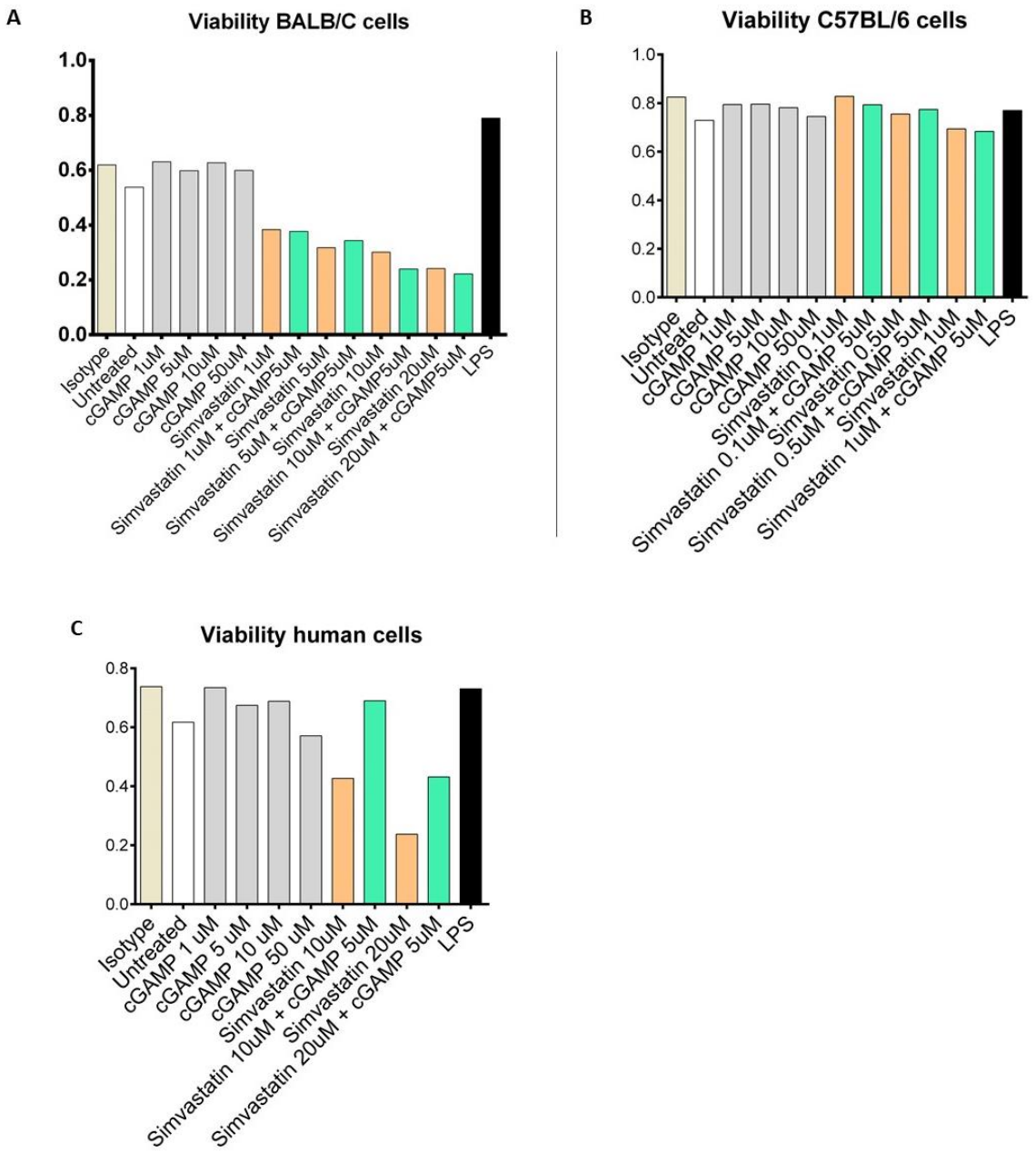

Figure s2. Bar charts of dendritic cell viability after stimulation with nystatin and 2'3'-cGAMP **A)** BMDCs from C57BL/6 strain **B)** BMDCs from BALB/c strain **C)** human moDCs